

2012•2013
FACULTEIT GENEESKUNDE EN LEVENSWETENSCHAPPEN
*master in de biomedische wetenschappen: klinische
moleculaire wetenschappen*

Masterproef

The menstruating mouse model for preclinical endometriosis research
Optimization of the decidualization process, nerve fiber detection and nocifensive behavior identification

Promotor :
dr. Nathalie GEURTS

Promotor :
prof. dr. THOMAS D'HOOGHE
Chloë Goossens

Copromotor :
dr. AMÉLIE FASSBENDER
ONBEKEND

Masterproef voorgedragen tot het bekomen van de graad van master in de biomedische wetenschappen, afstudeerrichting klinische moleculaire wetenschappen

De transnationale Universiteit Limburg is een uniek samenwerkingsverband van twee universiteiten in twee landen: de Universiteit Hasselt en Maastricht University.



Universiteit Hasselt | Campus Hasselt | Martelarenlaan 42 | BE-3500 Hasselt
Universiteit Hasselt | Campus Diepenbeek | Agoralaan Gebouw D | BE-3590 Diepenbeek



Maastricht University

2012•2013

FACULTEIT GENEESKUNDE EN
LEVENSWETENSCHAPPEN

*master in de biomedische wetenschappen: klinische
moleculaire wetenschappen*

Masterproef

The menstruating mouse model for preclinical
endometriosis research

Optimization of the decidualization process, nerve fiber
detection and nocifensive behavior identification

dr. Nathalie GEURTS

Promotor :
prof. dr. THOMAS D'HOOGHE

Copromotor :
dr. AMÉLIE FASSBENDER
ONBEKEND

Chloë Goossens

*Masterproef voorgedragen tot het bekomen van de graad van master in de biomedische
wetenschappen, afstudeerrichting klinische moleculaire wetenschappen*

Table of contents

TABLE OF CONTENTS	I
PREFACE	III
ABBREVIATIONS	V
ABSTRACT	VII
SAMENVATTING.....	IX
INTRODUCTION.....	1
1 Endometriosis.....	1
1.1 Etiology	1
1.1.1 Theories suggesting a uterine origin of endometriosis.....	1
1.1.2 Theories suggesting an extra-uterine origin of endometriosis	1
1.2 Pathogenesis	2
1.2.1 Survival of ectopic endometrial cells.....	2
1.2.2 Attachment and invasion of ectopic endometrial cells	3
1.2.3 Growth and development of ectopic endometrial tissue.....	3
1.3 Endometriosis-associated pain	4
1.4 Diagnosis and treatment	4
2 Animal models of endometriosis	5
2.1 Primate model	5
2.2 Rodent models.....	5
2.2.1 Menstruating mouse model	6
3 Research goals and experimental setup.....	7
MATERIALS AND METHODS.....	9
1 Animals	9
1.1 Ethics	9
1.2 Husbandry	9
2 Menstruating mouse model.....	9
2.1 Surgical procedures.....	9
2.2 Ovariectomy.....	9
2.3 Vaginal smear	9
2.4 Progesterone pellet	10
2.5 Hormonal regime	10
2.6 Optimization of decidualization process.....	11
2.6.1 Vaginal injections.....	11
2.6.2 Laparoscopic injections	11
2.6.3 Laparotomic injections	12
2.7 Tissue isolation and fixation	12
2.8 Microscopic evaluation of decidualization.....	12
2.9 H&E staining	12
2.10 Hormone measurements	13
2.10.1 Progesterone measurements	13
2.10.2 Estrogen measurements.....	13
2 Immunohistochemistry.....	14
2.2 Optimization PGP9.5 staining.....	14
2.2.1 REAL detection kit.....	14

2.2.2	NBT/BCIP.....	14
3	Pain tests.....	15
3.2	Optimization of pain tests.....	15
3.2.1	Hot water test	15
3.2.2	Acetone test.....	16
3.2.3	Von Frey hair test	16
3.2.4	Running wheel test	16
4	Statistical analysis.....	16
RESULTS.....		17
1	Optimization of the decidualization process	17
1.1	Uterine expansion and morphologic alterations characterized the decidualization process.....	17
1.2	Bicornuate decidualization was facilitated by all three intrauterine oil delivery methods	18
1.3	The endometrial surface area of decidualized uteri was comparable between the three intrauterine oil delivery groups	19
1.4	Laparotomic and laparoscopic injections differed in mortality and inflammatory response.....	20
1.5	Vaginal smears monitored the hormone sensitization and the induced bleeding	20
1.6	E2 and P4 circulating serum concentrations.....	21
1.6.1	The hormonal sensitization was reflected in the E2 and P4 serum concentrations.....	21
1.6.2	No differences in E2 or P4 serum concentrations were observed in animals that developed or failed to develop a decidualized endometrium	22
2	Optimization of the staining protocol for PGP9.5	22
2.1	Non-specific signal accompanied the visualization of PGP9.5 with the REAL Detection kit.....	23
2.2	PGP9.5 visualization using the chromogenic pair NBT/BCIP.....	23
2.2.1	Tris-HCl supplemented with EDTA heat retrieval produced excessive staining	23
2.2.2	Citrate heat retrieval and a 1:1000 antibody dilution best detected PGP9.5.....	24
2.2.3	Fast Red or hematoxylin counterstaining decreased the contrast with the NBT/BCIP chromogenic reaction.....	25
3.	Influence of CFA-induced abdominal pain on the nocifensive behavior of animals... 26	
3.1	The locomotive activity was not affected by CFA-induced abdominal pain.....	26
3.2	A minor effect on the temperature sensitivity was observed in relation to CFA-induced abdominal pain.	26
3.3	The mechanical sensitivity of animals tended to be affected by CFA-induced abdominal pain	27
DISCUSSION.....		29
CONCLUSION AND SYNTHESIS		38
REFERENCES.....		41
SUPPLEMENTAL INFORMATION		47

Preface

During the past eight months I was able to perform my senior internship in the lab of experimental gynecology at the KU Leuven. During this internship I grew tremendously as a researcher and was stimulated to explore different aspects of scientific research. For this reason, I would like to express some words of gratitude to several persons who helped me and stood by my side along the way.

First of all I would like to thank my promoter Prof. dr Thomas D'Hooghe for allowing me to perform my internship in his lab. Your intense knowledge concerning endometriosis was very inspiring and I also thank you for your constructive criticism during the endometriosis meetings.

Secondly, my co-promoter dr Amelie Fassbender also deserves a sincere word of appreciation. Amelie, thank you for all the times you read and corrected my thesis. I also want to thank you for providing good guidance. You introduced me to new techniques and stimulated me to believe in myself. Another thank you goes out to my daily supervisor Ms. Daniëlle Peterse for allowing me to improve my skills in working with laboratory animals and for stimulating me to become an individual scientist. I also appreciate that you gave me the possibility to participate in the development of your research project.

Next, my institutional supervisor dr Nathalie Geurts and my second examiner dr Leen Slaets deserve some gratitude for taking the time to assess my obtained results and for encouraging me to further reflect on the data.

Katrien De Clercq, my fellow 'endometriosis'-master student: thank you so much! From day one we got along really well and it truly was a pleasure to share all of my days with you. I enjoyed all of our laughs and silly behavior (I'm 100% sure we laughed more than the average seven times a day). Additionally, you gave ear to my complaints when times were rough and also postulated many constructive suggestions that helped me to perfect my thesis.

Subsequently, I would like to thank Prof. dr Joris Vriens for introducing me to the field of animal behavior. Joris, I appreciate that you shared your knowledge with me and that you were always willing to answer my questions. The lab technicians and other staff members are also entitled to an honest thank you. All of you always answered my (abundant) questions very kindly and accompanied me through my experiments.

I would also like to thank my friends at both the KU Leuven and the UHasselt. Tine, Sigrid, Goedele and Kathi: thank you for the many 'fruitjespauzes' and laughs. Manolo and Jessica, you have been there throughout all of these years. Although we performed our internships at different institutions, I always enjoyed keeping you posted and seeing you again.

Lastly, I sincerely thank my family. Mama, papa, Sue and Joachim, you have always supported me during my university years and we shared both the ups and downs. Without all of you, I would not have been able to do this.

Abbreviations

17 β -HSD:	17 β -hydroxysteroid dehydrogenase
BCIP:	5-bromo-4-chloro-3-indolyl phosphate
BSA:	Bovine serum albumin
CFA:	Complete Freund's adjuvant
E2:	17 β -estradiol
EDTA:	Ethylenediaminetetraacetic acid
ELISA:	Enzyme-Linked Immuno Sorbent Assay
FCS:	Fetal calf serum
H&E:	Hematoxylin and eosin
HCl:	Hydrochloric acid
HIAR:	Heat induced antigen retrieval
IL:	Interleukin
KU Leuven:	Catholic University Leuven
MMM:	Menstruating mouse model
MMPs:	Matrix-metalloproteinases
NBT:	Nitro blue tetrazolium
NFDM:	Non-fat dry milk
NK:	Natural killer
Ovex:	Ovariectomy
P4:	Progesterone
PBS:	Phosphate buffered saline
PEG400:	Polyethylene glycol 400
PGP:	Protein gene product
SD:	Standard deviation
T50:	50% response threshold
TBS:	Tris-buffered saline
TIMPs:	Tissue inhibitors of MMPs
TNF- α :	Tumor necrosis factor-alpha
Tris-HCl:	Tris(hydroxymethyl) aminomethane hydrochloride
VEGF:	Vascular endothelial growth factor

Abstract

Although endometriosis is one of the most common gynecological diseases, its exact etiology and pathogenesis remain poorly understood. Endometriosis research commonly employs rodent models. However, the current models fail to precisely replicate the human disease. Furthermore, the time line of processes involved in the development of endometriotic lesions, such as neuroangiogenesis, has not been elucidated in these models. Accordingly, the standardization and characterization of the menstruating mouse model (MMM) could signify advancement in the field of preclinical endometriosis research. The MMM facilitates menstruation by combining sensitization of ovariectomized animals towards estrogen and progesterone with the induction of a decidualization stimulus. In prospect of the standardization of this new model for endometriosis, this study comprised (i) the optimization of the decidualization protocol of the MMM; (ii) the improvement of the immunostaining for protein gene product (PGP) 9.5; and (iii) the assessment of nocifensive behavior related to abdominal pain.

The first part of this study hypothesized that laparotomic or laparoscopic intrauterine oil delivery would result in 100% decidualized endometrium in both uterine horns while performing decidualization by vaginal injection would only result in the formation of bicornuate deciduas in 50% of the animals. Results indicated that vaginal injections caused bicornuate decidualization in 30% of the animals and that the percentage of bicornuate decidualization amounted to 88% in the laparotomic and to 84% in the laparoscopic injection group. Furthermore, a significant increase in relative uterine weight (p -value <0.01 and 0.05) and endometrial surface area (p -value <0.05) compared to the sham group, accompanied laparotomic and laparoscopic injections. Although laparotomy and laparoscopy were equally capable of causing decidualization, comprehension of each technique's side effects rendered laparoscopy the most optimal intrauterine oil delivery method. The second aim encompassed the evaluation of different chromogens, heat retrieval methods and primary antibody dilutions for the PGP9.5 immunostaining. Results indicated that nerve fibers were best detected in the peritoneum after citrate heat retrieval, an antibody dilution of 1:1000 and detection with the chromogenic pair nitro blue tetrazolium/5-bromo-4-chloro-3-indolyl phosphate (NBT/BCIP). Finally, this study assessed the nocifensive behavior of animals in response to abdominal pain, to provide an indication of this behavior for endometriosis-associated pain. Pain in the lower abdomen was induced by subcutaneous injections with complete Freund's adjuvant (CFA) and the behavior of the animals was appraised using pain tests examining the temperature sensitivity (acetone test and hot water test), mechanic sensitivity (von Frey hair test) and locomotive activity (running wheel test) of the animals. Results showed no significant differences in nocifensive behavior regarding all of these tests.

Taken together, the current study performed different optimization steps in anticipation of the standardization and subsequent validation of the MMM as preclinical endometriosis model. In addition, the outcomes of these optimization steps can be used in future studies on the early development of endometriosis in the MMM.

Samenvatting

Hoewel endometriose een veelvoorkomende gynaecologische aandoening is, zijn haar etiologie en pathogenese niet volledig gekend. Vaak wordt er beroep gedaan op knaagdiermodellen, ondanks dat deze modellen de humane ziekte niet nauwkeurig genoeg nabootsen. Daarnaast werd in deze modellen het ontstaan van belangrijke pathogene endometriosegerelateerde processen, zoals neuroangiogenese, nog niet onderzocht. De standaardisatie van het menstruerend muismodel (MMM) zou een belangrijke vooruitgang betekenen voor het preklinisch endometrioseonderzoek. Dit model berust op de inductie van menstruatie door het toedienen van estradiol en progesteron in combinatie met een decidualisatiestimulus. Met de standaardisatie van dit nieuwe model in het vooruitzicht werden volgende stappen ondernomen: (i) de optimalisatie van het decidualisatieprotocol van het MMM; (ii) de verbetering van de 'protein gene product' (PGP) 9.5 immunokleuring; en (iii) de beoordeling van het nocifensief gedrag ten opzichte van abdominale pijn.

Het eerste deel van deze studie stelde als hypothese dat laparotomische of laparoscopische intra-uteriene olie injecties zouden resulteren in 100% bicornuate decidualisatie, terwijl vaginale injecties slechts tweehoornige decidualisatie zouden faciliteren in 50% van de dieren. Er werd aangetoond dat vaginale injecties in 30% van de dieren tweehoornige decidualisatie veroorzaakten en dat het percentage van bicornuate decidualisatie 88% bedroeg in de laparotomie- en 84% in de laparoscopiegroep. Verder werd in de laparotomie- en laparoscopiegroep een significante verhoging waargenomen ten opzichte van de controlegroep in relatief uterusgewicht (p -waarde < 0.01 en 0.05) en endometriaal oppervlaktegebied (p -waarde < 0.05). Ook werd aangetoond dat laparoscopie en laparotomie een equivalente hoeveelheid gedecidualiseerd weefsel opleverden, hoewel laparoscopie als optimale intra-uteriene olie injectietechniek aangeduid werd na het afwegen van de verschillende voor- en nadelen van beide technieken. Als tweede objectief werden verschillende chromogenen, 'heat retrieval' methoden en primaire antilichaamverduunningen van de PGP9.5 immunokleuring geëvalueerd. Zenuwvezels werden het best gedetecteerd na citraatafhankelijke 'heat retrieval', een primair antilichaamverduunning van 1:1000 en visualisatie doormiddel van het chromogeenpaar 'nitro blue tetrazolium/5-bromo-4-chloro-3-indolyl phosphate' (NBT/BCIP). Als laatste bestudeerde deze studie het nocifensief gedrag van dieren als respons op abdominale pijn om een indicatie te geven over dit gedrag betreffende pijn in endometriose. Abdominale pijn werd geïnduceerd doormiddel van subcutane injecties met complete Freund's adjuvant (CFA) en het gedrag van de dieren werd geëvalueerd aan de hand van pijntesten die temperatuur sensitiviteit (aceton test, hot water test), mechanische sensitiviteit (von Frey test) en locomotor functie (running wheel test) beoordeelden. De resultaten toonden geen significante verschillen in nocifensief gedrag met betrekking tot alle gebruikte testen.

Als conclusie werd gesteld dat verschillende optimalisatiestappen werden uitgevoerd om het MMM als preklinisch model voor endometriose te standaardiseren. Verder kunnen de resultaten van deze studie gebruikt worden in nieuwe studies over de vroege ontwikkeling van endometriose, gebruikmakend van het MMM.

1 Endometriosis

Endometriosis is one of the most common gynecological disorders, affecting approximately 10% of women in the reproductive age group and up to 50% of all infertile women (1, 2). Characteristic for this estrogen-dependent disease is the presence of endometrial-like tissue occurring at ectopic sites such as the pelvic peritoneum, the ovaries, the rectovaginal septum and in some cases even the pericardium, the pleura and the brain (1). The most important symptoms of endometriosis comprise infertility and pain. It is estimated that up to 50% of endometriosis patients is subfertile (any form of reduced fertility with prolonged time of unwanted non-conception) (3). Furthermore, endometriosis-associated pain typically arises as chronic pelvic pain in 90% of women suffering from painful menstruations (dysmenorrhea), in 42% of women suffering from pain during intercourse (dyspareunia) and in 39% of women suffering from non-menstrual pain (4, 5). The economic burden associated with endometriosis should also be considered as it is comparable to that of diabetes mellitus and Crohn's disease (6). Accordingly, endometriosis is perceived as a disease that imposes a significant burden on endometriosis patients' quality of life and on health costs (7, 8).

1.1 Etiology

Although endometriosis has been acknowledged over a hundred years ago, its exact etiology remains unknown. In an attempt to address the disparate observations regarding the pathogenesis of endometriosis, different theories have been composed (9).

1.1.1 Theories suggesting a uterine origin of endometriosis

The theory of retrograde menstruation, as defined by Sampson, is the most accepted theory of endometriosis. It states that during menstruation, flow-back of endometrial tissue through the fallopian tubes into the peritoneal cavity results in implantation and growth as endometriotic lesions (10). An increased prevalence of endometriosis in patients with congenital outflow obstruction and in non-human primate models with iatrogenic outflow obstruction argues in favor of this implantation theory (11, 12). Although Sampson's theory is widely accepted, a discrepancy between the occurrence of endometriosis and that of retrograde menstruation exists, questioning the integrity of the retrograde menstruation theory (13). An alternative theory, the benign metastasis theory, states that lymphatic or hematogenous dissemination forms the basis of ectopic endometrial implantation (10). This theory is supported by the presence of endometriotic lesions at distant sites such as the lung (14).

1.1.2 Theories suggesting a extra-uterine origin of endometriosis

Findings of endometriosis in patients without menstrual endometrium led to the emergence of theories suggesting an extra-uterine origin of endometriosis (15). The theory of coelomic metaplasia entails that endometrial tissue arises from metaplasia of the coelomic membrane (9).

This theory clarifies the origin of endometriosis in the absence of menstruation and can explain the occurrence of endometriosis in rare places, men and adolescent girls (14, 16-18). The induction theory extends the coelomic metaplasia theory with the assumption that endogenous stimuli, such as hormonal or immunologic factors, stimulate endometrial differentiation of cells from the peritoneal lining (9). The observation that endometriosis can occur by serial changes from mesothelial cells supports this theory (19). Contrary to the induction theory, the embryonic rest theory states that residual cells from the embryologic Müllerian duct migration still have the capacity to transform into endometriotic lesions under the influence of estrogen (20). Indeed, a twofold increased risk of endometriosis has been reported by epidemiological studies in women exposed to diethylstilbestrol *in utero* (21). Finally, the possibility of extra-uterine stem/progenitor cells differentiation into endometrial tissue has recently been explored. Bone marrow mesenchymal stem progenitors and endothelial progenitors are suggested as cell lineage candidates (22).

Each etiologic theory of endometriosis is supported by scientific findings, of which the retrograde menstruation theory is substantiated by the largest amount of evidence. However, a unifying theory remains elusive, demonstrating the complex nature of endometriosis.

1.2 Pathogenesis

The exact pathogenesis of endometriosis also remains poorly understood (23). Recently, a variety of critical steps have been postulated to be involved in the development of endometriotic lesions. Since Sampson's theory is supported by the most abundant data, the proposed mechanisms are mainly based on this hypothesis (20).

1.2.1 Survival of ectopic endometrial cells

An important aspect in the development of endometriotic lesions is the survival of endometrial cells outside of their physiological environment. Different aspects are thought to assist endometriotic lesions in their growth. For instance, the eutopic endometrium of endometriosis patients is altered in comparison to that of healthy women (20). An increased expression of anti-apoptotic factors and a decreased expression of pro-apoptotic factors have been observed in the eutopic endometrium of endometriosis patients (20, 24). Additionally, the observed genomic alterations may be consequent to epigenetics and/or oxidative stress (25). The fact that endometriosis is hereditary in 51% of the cases and that locus 7p15.2 has recently been linked to an increased risk of endometriosis further strengthens the genetic component (26).

The immune system plays an important role in endometriosis and has been ascertained as a causative factor in the survival of the sloughed endometrial tissue. A defective immune clearance is likely to promote the survival of endometrial tissue in the peritoneal cavity (20). The peritoneal fluid of endometriosis patients is marked by a high number of white blood cells and macrophages, indicating an increased inflammatory state (27). Furthermore, a malfunction of natural killer (NK) cells in combination with an impairment of the T-cell mediated cytotoxicity could facilitate the escape of ectopic endometrial tissue from the immune system (20). Taken together, the

inadequate immune surveillance in combination with the decreased apoptosis probably allows the survival of endometrial cells in the peritoneal cavity (27).

1.2.2 Attachment and invasion of ectopic endometrial cells

Attachment of ectopic endometrial cells to the mesothelial cell lining of the peritoneum is established through endometrial stromal cells. However, the exact mechanisms underlying endometrial-mesothelial cell adhesion remain unresolved (28). Also not negligible is the stimulation of the invasive growth by an increased expression of matrix-metalloproteinases (MMPs) and decreased expression of tissue inhibitors of MMPs (TIMPs). Furthermore, an additional upregulation of cytokines such as interleukin (IL)-1 and tumor necrosis factor-alpha (TNF- α) may also create an environment that promotes endometrial cell implantation (27, 29).

1.2.3 Growth and development of ectopic endometrial tissue

A range of mechanisms is likely involved in the growth and development of endometriotic lesions (20). Firstly, the eutopic endometrium of endometriosis patients does not only differ from that of healthy women, there are also fundamental differences detected within the ectopic endometrium of endometriosis patients (30). Changes in the hormonal environment have been denoted as stimulatory for the growth of ectopic endometrial tissue. An increased production of estrogen, prostaglandins, and pro-inflammatory cytokines by ectopic endometrial tissue is observed (31). Furthermore, a differential expression of estrogen receptors and progesterone (P4) receptors, an increased expression of aromatase (an enzyme that catalyses the conversion of androgens to estrogens) and a decreased expression of 17 β -hydroxysteroid dehydrogenase (17 β -HSD) type 2 (an enzyme responsible for the inactivation of 17 β -estradiol (E2) to estrone) are also present in endometriotic lesions (32-34).

Secondly, self-sustainability is a crucial feature for the growth and development of endometriotic lesions. In recent years, angiogenesis has been found essential for the development and maintenance of lesions (35). Indeed, a web of blood vessels and neovascularization (vascularization in abnormal quantity or in abnormal tissue) frequently surrounds endometriotic lesions (36). Additionally, lymphangiogenesis (formation of lymphatic vessels from pre-existing lymphatic vessels, in a method believed to be similar to angiogenesis) and neurogenesis (development of nerves, nervous tissue, or the nervous system) are also involved in the development and maintenance of endometriotic lesions. The implication that lymphangiogenesis is important in endometriosis is substantiated by the finding of a high density of lymph vessels in endometriotic lesions (37). Neuronal tissue also pervades human endometriotic lesions (4, 37). Different types of nerve fibers (sensory Ad, sensory C, cholinergic and adrenergic nerve fibers) play a part in the innervation of peritoneal endometriotic lesions (38). Although neurogenesis has already been studied in endometriosis, the exact origin of nerve fibers in endometriotic lesions remains mostly elusive.

1.3 Endometriosis-associated pain

Endometriosis patients commonly suffer from pain, of which the symptoms vary from person to person (4). The spectrum of pain types ranges from 'simple' severe dysmenorrhea to chronic pelvic pain and other co-morbid pain conditions (39). In concordance with the etiology of endometriosis itself, the exact etiology of endometriosis-associated pain also remains largely unknown (4). However, it has been postulated that cyclic bleeding of the lesions, pelvic inflammation and neuroangiogenesis may give rise to pain in endometriosis (39). The presence of steroid receptors on endometriotic lesions in combination with the observation of bleeding from the ectopic lesions, favor the assumption that pain is correlated to cyclic bleedings (32, 40, 41). As noted before, pelvic inflammation is often observed in endometriosis patients (4). The existing macrophage activation leads to the production of chemokines, which in turn activate leukocytes. These leukocytes are known to stimulate pro-inflammatory molecules such as prostaglandins. Hereafter, these prostaglandins can directly activate nociceptors on nerve fibers (42-44). Recently, the process of neuroangiogenesis gained interest with regard to pain in endometriosis. Neuroangiogenesis is a process through which ectopic implants recruit their own neural and vascular supplies. The idea originated from the finding that neurogenesis and angiogenesis are stimulated by the same molecules such as vascular endothelial growth factor (VEGF) (4). Although neuroangiogenesis received a lot of attention, still little is known about this process in endometriosis-associated pain.

1.4 Diagnosis and treatment

Diagnosing endometriosis is currently performed through laparoscopic identification of ectopic endometrial-like tissue (1). Classification of the disease according to the revised American Fertility Society classification system (stage I to IV or minimal to severe) is based on the acquired information during laparoscopic surgery concerning the morphology and depth of the implants, the presence, place and type of lesions, and the presence, place and type of adhesions (45). Although laparoscopy is considered the golden standard, it sometimes fails to detect very small lesions and lesions at unconventional locations (46). Another diagnostic method comprises ultrasonographic examination of lesions. This technique only detects ovarian endometriotic cysts and some deeply infiltrative endometriotic nodules. Accordingly, ultrasound is not adequate for the diagnosis of peritoneal endometriosis (8). Furthermore, as endometriosis is difficult to diagnose due to the overlap of the symptoms with other disorders, an average delay of eight years precedes an accurate diagnosis. Five to six of these years can be attributed to a delay in the search of medical help and the remainder to obtaining the correct diagnosis (47).

Treatment options are directed against endometriosis itself, against endometriosis-associated pain or against endometriosis-related infertility. Endometriosis as such is often treated with surgery and medical therapy (7). Surgery aims to remove all visible endometriotic lesions, but as it does not influence the underlying mechanisms of the disease, recurrences of endometriotic lesions are common (48). Contrary, the current medical treatments focus on altering the hormonal milieu in order to create an environment, suboptimal for the growth and maintenance of the lesions. Still, these medications have many side effects and their efficiency is not ideal (8, 48). It has been indicated that the underlying mechanisms of endometriosis need to be clarified to improve

diagnostic tools and treatment strategies (7). Indeed, in recent years the pathogenesis and pathophysiology of endometriosis are slowly being uncovered and new, more targeted therapies are being developed, e.g. aromatase and angiogenesis inhibitors (49).

2 Animal models of endometriosis

To date, the lack of reliable noninvasive methods for detecting early endometriosis in humans renders the study of the early development of endometriosis in women unfeasible and unethical. This contributes to the common employment of animal models in endometriosis research (50). Additionally, animal models are also very valuable for the pharmaceutical industry where they serve as preclinical models to evaluate new screening and therapeutic tools (51).

2.1 Primate model

The primate model is considered the most relevant animal model for the study of endometriosis as non-human primates show many reproductive similarities to humans (50). It has long been noted that baboons have a comparable reproductive anatomy and physiology. Furthermore, vast resemblances in the cyclic steroid hormone levels are shown throughout the menstrual cycle of humans and baboons (52, 53). In addition, the presence of a menstrual cycle in non-human primates allows the development of spontaneous endometriosis in these animals (54). In primate models of endometriosis, the relationship between the establishment of endometriosis and the immune system is commonly studied (52).

Although the primate model comes across as the perfect endometriosis model, there are disadvantages associated with the employment of non-human primates. Trained personnel and an adapted infrastructure are essential when working with these animals, resulting in high costs. Ethical considerations have also been reported as a limiting factor in the use of nonhuman primates for research in reproduction and endometriosis (50-52).

2.2 Rodent models

Two different rodent models of endometriosis can be distinguished: the heterologous model and the homologous model (52, 54, 55). On the one hand, the heterologous model is based on xenotransplantation of human endometrial tissue into immune deficient mice by means of laparotomy. Evaluation of the responsiveness of ectopic lesions towards steroid hormones and the assessment of the early development of endometriosis are regularly evaluated in the heterologous model (54). On the other hand, the homologous model relies on the transplantation of endometrial fragments from syngeneic animals into immune competent recipients by means of surgery or intraperitoneal injections (52). In this model, the effect of immune-modulating drugs and anti-inflammatory agents in endometriosis is commonly studied (55).

At present, a need for new, standardized, affordable preclinical models for the development of therapeutic agents directed against endometriosis exists (51). In this setting, rodent models are very attractive as rodents have the advantage of being easy to handle and they also are

inexpensive to maintain (7). Although the vast majority of preclinical studies are performed on rodent models, their suitability in endometriosis research is disputed. Disadvantageously, the current rodent models do not succeed in completely mimicking the human disease (51). General limitations of the employment of rodents in endometriosis research are the lack of similar reproductive physiology and anatomy compared to that of humans. Differences can be observed between the estrous cycle of rodents and the menstrual cycle of humans. Both reproductive cycles rely on the presence of estrogen and progesterone (56). However, decidualization (morphological and biochemical changes of the endometrial stromal compartment that bestow the endometrial characteristics essential for pregnancy) differs drastically in both cycles. In the menstrual cycle, endometrial stromal cells differentiate into decidualized cells in response to an increased progesterone production. When blastocyst implantation is absent, the decidualized tissue is shed during menses (57). Contrary, in the estrous cycle decidualization only occurs after blastocyst implantation into the endometrium (56). Additionally, the estrous cycle of rodents is characterized by complete re-absorption of the endometrial lining without any external signs (58). Therefore, the absence of menstruation in rodents makes the development of spontaneous endometriosis in these animals impossible (52).

Apart from general limitations, each of the rodent models has its own restrictions with respect to the human disease. Concerning the heterologous model, the deficient immune system of the employed animals does not reflect the human immunologic situation (55). Furthermore, the use of the heterologous model in the pharmaceutical industry would possibly be problematic since fresh human tissue is required. The homologous model is not deemed very suitable to investigate endometriosis since the cause of endometriosis possibly relies on the properties of the eutopic endometrium itself (20, 52). Additionally, in most studies employing this model, the endometrium was not separated from the myometrium before transplantation (55). This results in the formation of implants that are surrounded by a layer of myometrial smooth muscle tissue. Myometrial smooth muscle tissue is however, not a basic feature of most human endometriotic lesions (51).

2.2.1 Menstruating mouse model

The current problems faced when working with rodent models in endometriosis research can be overcome by developing more suitable models. An important characteristic of a suitable animal model involves precise modeling of the human disease. In endometriosis research this encompasses mimicking both the etiology and the pathogenesis. To simulate the process of retrograde menstruation as closely as possible, a menstruating mouse model (MMM) has recently been adapted for the use in endometriosis research (unpublished data from Edinburgh University) (59). The adaptation involves the implantation of decidualized premenstrual or early menstrual endometrium from a donor mouse into the peritoneal cavity of a syngeneic recipient mouse (59). The MMM itself has been developed to evaluate the mechanisms underlying menstruation (60). The model is accomplished by inducing decidualization through the instillation of oil into the uterine lumen of the hormone-sensitized animals. The animals' hormone sensitization can be effectuated by either inducing pseudo-pregnancy or by priming ovariectomized mice by the administration of estrogen and progesterone (56, 57). Breakdown of the decidualized tissue is only observed

simultaneous with a drop in progesterone level, resulting in overt menstruation-like bleeding (61, 62). Even though research within the MMM is fairly new, different studies indicated that murine menstruation occurs equivalently to menstruation in humans. The main event of bleeding can be observed in this model, although microscopic endometrial breakdown was observed more clearly (56). Bleeding has been reported to peak at 24h after progesterone withdrawal, when the decidua is separated from the rest of the endometrium (61). Additionally, it has been shown that, similar to humans, dynamic remodeling of endometrial vasculature is associated with endometrial breakdown and repair and that breakdown is initiated by increases in the MMP expression (63, 64). The occurrence of leukocyte infiltration further indicated the correspondence between the MMM and human menstruation (57, 61). In spite of the extent of data on the MMM and its recent adaptation for endometriosis, it has not yet been thoroughly characterized, standardized and validated for the use in endometriosis research. Furthermore, the early development of endometriosis has never been studied in this model.

Besides modeling the process of retrograde menstruation as precisely as possible in rodents, the MMM has additional advantages. Firstly, the possibility to establish knockout mice within this model exists. Secondly, the MMM does not rely on human tissue. This reduces the biological variation in menstrual cycle of the obtained tissue and makes it easier to apply the model in the pharmaceutical industry. A critique on the MMM covers the possibility that the cause of endometriosis may rely on the properties of the eutopic endometrial tissue itself (20).

Although the MMM for endometriosis seems very promising, currently the yield of decidualized endometrial tissue from donor animals is low. Furthermore, the lesion development in this model is also not optimal. The retrieved lesions were shown small and did not survive longer than 14 days (59). Moreover, only 40% of the recovered lesions in recipient mice have been histologically confirmed as endometriotic lesions, defined by the presence of endometrial glands, stromal and epithelial cells (unpublished data from Edinburgh University). These data indicate a need to improve of the MMM in endometriosis research. In addition, standardization of the MMM for endometriosis would increase the reproducibility of preclinical studies within this model (51).

3 Research goals and experimental setup

The insufficient knowledge on the etiology and pathogenesis of endometriosis in combination with the lack of good preclinical endometriosis models limits the pharmaceutical industry to ameliorate translation towards endometriosis patients. The faced translational challenge could be obviated by the development of validated and affordable preclinical animal models that realistically represent the different facets of the human disease. However, the currently used rodent models fail to mimic endometriosis closely enough. Therefore, the recent development of the MMM for endometriosis research could signify advancement in the field of animal models for endometriosis. To promote translational confidence in this model, validation of the MMM for endometriosis is necessary. Hence, characterization of processes important for the development of endometriotic lesions and endometriosis-associated pain in this model is needed. Nevertheless, before characterization can take place, different aspects are in need for optimization.

Objective 1: Improvement of the decidualization process in the MMM

The decidualization protocol, as currently used by our associates of Edinburgh University, merely causes a decidualized endometrium in 50% of the donor animals and this in only one uterine horn. However, to decrease the number of donor animals that are needed for the MMM in endometriosis setting, more decidualized endometrial tissue is desirable. In order to accomplish this, the decidualization process needs to be optimized. For this purpose, the effect of the different routes for intrauterine oil delivery will be examined. A comparison between the outcome of intrauterine oil delivery through vaginal injections, laparoscopic injections and laparotomic injections will be performed and the effect on the generation of deciduas will be evaluated. It is hypothesized that laparotomic or laparoscopic intrauterine oil delivery will result in 100% decidualized endometrium in both uterine horns while performing decidualization by vaginal injection will only result in bicornuate decidualization in 50% of the animals.

Objective 2: Optimization of visualization technique for nerve fibers

The role of neurogenesis in the development of endometriotic lesions and the role of neuroangiogenesis in endometriosis-associated pain recently gained a lot of interest. However, a lot of uncertainties are still present concerning the underlying mechanisms. In order to evaluate the presence of nerve fibers during the development of endometriotic lesions, immunohistochemical methods can be used. The identification of neurons can be achieved by using antibodies directed against protein gene product (PGP) 9.5, a pan neuronal marker. To acquire the optimal staining protocol, optimization of the immunohistochemical staining is needed. Therefore, the effect of different antigen retrieval methods, concentrations of the primary antibody and chromogens on the immunostaining will be examined.

Objective 3: Determination of nocifensive behavior related to endometriosis-associated pain

Although pain in endometriosis has been acknowledged as important, neither the pathogenesis nor the etiology of endometriosis-associated pain have been fully elucidated. To increase our knowledge on endometriosis-related pain, pain can be assessed in endometriosis animal models. However, currently, no validated pain test to measure pain related to endometriosis in rodent models exists. No pain tests have been performed on the lower abdomen of rodents, even though endometriosis-associated pain is commonly experienced most intensely at places with the highest occurrence of lesions (39). Therefore, to accurately evaluate pain in an endometriosis model, the locomotive activity, mechanical sensitivity and temperature sensitivity of the animals will be studied using a number of tests such as the running wheel test, the von Frey hair test, the hot water test and the acetone test. This novel approach requires determination of the nocifensive behavior (behavior induced by stimuli that activate the nociceptive sensory apparatus) of the animals. For this reason, pain tests will be performed to assess the response to noxious and innocuous stimuli, before and after an injection with complete Freund's adjuvant (CFA). All pain tests will be performed in collaboration with master student Katrien De Clercq from the Catholic University Leuven (KU Leuven).

Materials and methods

1 Animals

1.1 Ethics

All animal experiments were approved by the Ethical committee for animal experiments at the KU Leuven, Belgium.

1.2 Husbandry

Forty-five female 8 weeks old C57BL/6 mice were ordered from the internal breeding stock of the KU Leuven (n=5) or Janvier (n=40; Saint Berthevin Cedex, France). Five mice were housed per cage in rooms with a temperature of $23 \pm 1.5^{\circ}\text{C}$ and humidity between 40-60% with a 14:10 hour light-dark cycle. The mice were fed *ad libitum* with food pellets and water.

2 Menstruating mouse model

2.1 Surgical procedures

Surgeries such as ovariectomy, hormone pellet implantation and removal, and the induction of decidualization were performed under isoflurane-induced anesthesia (between 1 and 2% Iso-Vet; Eurovet, Bladel, The Netherlands). Prior to the surgical procedure, the appropriate area was shaved and disinfected using an iodine based solution (BDH Prolabo – VWR International, Amsterdam, The Netherlands). After surgery, the skin incision was sutured with a 6-0 polyglycolic acid thread (Dexon II, Davis1Geck, Gosport, UK) and a subcutaneous injection of 0.05 mg/kg buprenorphine (Vetergesic, Ecuphar, Breda, The Netherlands) diluted in saline (0.9% NaCl; Viaflo, Baxter, Utrecht, The Netherlands) was given on two consecutive days to induce painkilling.

2.2 Ovariectomy

To exclude aberrations in the hormonal environment due to the endogenous hormone production of the animals, mice were ovariectomized. The mice were anesthetized and ovariectomy was performed bilaterally. Briefly, a dorsal midline skin incision was made caudal to the posterior border of the ribs. Subsequently, the peritoneum was incised at the level of the ovaries. The end of the uterine horn was fixed through the opening followed by clamping of the fallopian tubes. Hereafter the ovaries were removed.

2.3 Vaginal smear

The estrous cycle of ovariectomized animals was staged by vaginal cytology. Vaginal smears were conducted daily between 08:30h and 10:00h. The animal was secured and 50 μl phosphate buffered saline (PBS, pH 7.4; Gibco, Invitrogen, Ghent, Belgium) was applied into the vagina. The vagina was gently flushed five times with PBS to ensure that a sufficient number of cells were taken. The final flush was collected and placed onto a glass microscope slide. Hereafter, the vaginal fluid was

examined under a light microscope (Leica DM LB, Leica Microsystems, Wetzlar, Germany) with 10x/0.30 PL fluotar objective (Leica Microsystems) at low illumination and without the use of the condenser lens to assure good contrast. If the smear was desiccating, a small amount of PBS was added. Stages of the estrous cycle were determined as described by *Caligioni* (65) (Supplementary data figure 1):

- Proestrus – predominance of nucleated epithelial cells in clusters or separately, some cornified cells may be observed
- Estrus – abundance of cornified squamous epithelial cells in clusters
- Metestrus – a mix of cell types is present, predominantly leucocytes and few nucleated epithelial and/or cornified squamous epithelial cells
- Diestrus – predominance of leucocytes

On day 13 of the menstruating mouse protocol (Figure 1), immediately prior to sacrificing the animals, a final vaginal smear was obtained. The smear was macroscopically examined to determine whether menstrual blood was present.

2.4 Progesterone pellet

Pellets were prepared as adapted from *Milligan and Cohen* (66). In short, silastic tubes (outer diameter 3.18mm; Dow Corning, Seneffe, Belgium) were filled with progesterone (Sigma-Aldrich, Bornem, Belgium) and the ends of the tubes were sealed with multipurpose sealant (Dow Corning), yielding a functional length of 1cm for each pellet. Twenty-four hours prior to implantation, pellets were placed in PBS supplemented with 5% fetal calf serum (FCS; Gibco) and kept at 37°C in order to induce pumping of the progesterone.

2.5 Hormonal regime

One week after ovariectomy, mice received subcutaneous injections of 100ng E2 on three consecutive days. E2 dilutions were made one day prior to the series of three injections. A stock solution of 1mg E2 in 1ml 96% ethanol (VWR, Leuven, Belgium) was diluted 1000 times in arachis oil to obtain the 100ng concentration. After the animals had a three day resting period, a P4 pellet was subcutaneously implanted in the neck of each animal. In short, a small incision was made in the loose skin of the mouse's neck, and a pocket was bluntly dissected. The hormone pellet was gently installed using forceps. The incision was subsequently closed by a suture. Coinciding with the pellet placement, the mice received subcutaneous injections of 5ng E2 on the subsequent three days. The 5ng concentration was attained through a 20 times dilution of the stock into 96% ethanol and a subsequent 1:1000 dilution in arachis oil. After three days, the P4 pellet was removed to initiate P4 withdrawal.

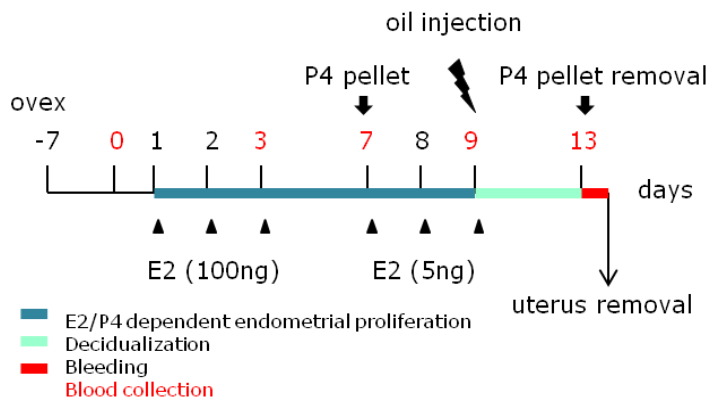


Figure 1: **Experimental setup of the MMM.** Mice were ovariectomized and hormonal sensitization was performed by the injection of E2 (100ng and 5ng) and the implantation of a P4 pellet. Decidualization was induced by injecting oil into the uterus by means of different techniques including vaginal injections, laparoscopic injections and laparotomic injections. Five hours after the removal of the P4 pellet, endometrial bleeding was assessed and the uterus was isolated for macroscopic and morphologic evaluation. Blood samples were collected at day 0, 3, 7, 9 and 13 [MMM: menstruating mouse model, ovex: ovariectomy, E2: 17 β -estradiol, P4: progesterone].

2.6 Optimization of decidualization process

Concomitant with the last day of E2 treatment, 40 μ l of sesame oil (20 μ l per uterine horn) was introduced into the uterus to induce decidualization. Sesame oil was applied by means of vaginal, laparoscopic, and laparotomic injections. The animals were randomly assigned to one of the injection groups using computerized block randomization:

- Sham group (n=9) - the animals obtained the hormonal sensitization but did not receive the decidualization stimulus
- Vaginal injection group (n=10) - the animals underwent hormonal treatment and decidualization was achieved via vaginal injection of sesame oil
- Laparoscopic injection group (n=6; three animals died during the procedure) - the animals obtained hormonal treatment and received the decidualization stimulus by means of laparoscopy
- Laparotomic injection group (n=9; one animal died during the procedure) - the animals underwent hormonal treatment and the induction of decidualization was performed by means of laparotomy

2.6.1 Vaginal injections

The vaginal injections were performed by introducing a blunted 22G catheter (Insyte, Vialon, Becton Dickinson, Madrid, Spain) connected to a 1ml syringe (BD biosciences, San Jose, USA) into the uterine horn through the vaginal opening.

2.6.2 Laparoscopic injections

To insure that the animals were sufficiently anesthetized prior to the incubation, 1mg/kg medetomidine (Domitor; Pfizer, MA, USA) was given. Hereafter, the animals were secured in a supine position and intubated endotracheally with a 20G catheter, connected to a mechanical respirator (Rodent Ventilator; Harvard Apparatus, Holliston, USA) using 250 μ l air/stroke and 180 stokes/minute. The laparoscopic procedure was adapted from *Molinas et al* (67). In short, a 3.5mm abdominal incision was made caudal to the xyphoides appendix and the endoscope, connected to a single chip video camera and light source (Karl Storz, Tuttlingen, Germany), was introduced into

the peritoneal cavity. The endoscope was secured in a holder and the incision around the endoscope was closed with a 6-0 polyglycolic acid suture to prevent leakage. Hereafter, two 14G catheters (Insyte) were inserted under laparoscopic vision in the left and right flank of the mouse. Fixation of the uterine horn was achieved using a small grasper. A syringe containing sesame oil was introduced into the peritoneal cavity via the abdominal wall. Subsequently the sesame oil was injected into the middle of the uterine horn using the opening created by the removal of the ovaries as a passageway. The second uterine horn was treated equivalently.

2.6.3 Laparotomic injections

A dorsal midline skin incision caudal to the posterior rim of the ribcage was made. On both sides of the spine, at the level of the previously removed ovaries, the peritoneum was incised. The uterine horn was gently fixed through the incision and a syringe containing sesame oil was introduced into the middle of the uterine horn through the opening created by the removal of the ovaries. The oil was injected and the procedure was repeated for the second uterine horn.

2.7 Tissue isolation and fixation

The day of the sacrifice, the animals were weighted and five hours after the initiation of progesterone withdrawal the animals were sacrificed and the uterus was isolated. The weight of the uterus was recorded and hereafter the uterus was macroscopically assessed followed by separating the uterine horns and cutting them transversally through the middle. Cut uterine horns were fixed in 4% formaldehyde for a minimum of 24 hours followed by transference of the uteri onto PBS for one hour. After incubation, the samples were kept in 70% ethanol until paraffin embedding.

2.8 Microscopic evaluation of decidualization

Paraffin-embedded uterine tissue was cut into sections of 4 μ m at six standardized places along the horn using the HM 340 E Rotary Microtome (Mictrom International GmbH – Thermo Fisher Scientific, Walldorf, Germany). In short, the first section was made when both halves of the uterine horn in one paraffin block were broached. Subsequently, 650 μ m of tissue was trimmed and the second section was made. The trimming process was repeated before making a third section. Since each paraffin block contained two halves of one uterine horn, the three obtained sections accommodated six different places along the uterine horn. The uterine cross-sections were stained with a hematoxylin and eosin (H&E) staining (protocol in section 2.9) and visualization was performed with a Zeiss Axioskop Microscope (Carl Zeiss, Zaventem, Belgium) equipped with an Axiocam MRC5 (Carl Zeiss). Pictures of the horns were taken and the endometrial surface was delineated using Zen 2011 software (Carl Zeiss).

2.9 H&E staining

Slides were incubated at 55°C for at least one hour. Hereafter, deparaffinization and rehydration (2x 5min toluol (Labonord, Templemars, France); 2x 5min 100% ethanol (Fagron, Waregem, Belgium)) and washing steps were performed. Slides were incubated in Gill hematoxylin (Prosan, Merelbeke, Belgium) for four minutes after which the washing step was repeated. Subsequently the

slides were dipped in acid alcohol (1% HCl in 100% ethanol) and lithium carbonate (saturated in distilled water), alternately washing them. After a three minute incubation with eosin (Prosan), slides were quickly washed and dehydrated (2x 5min propanol (Fagron); 2x 5min toluol) before mounting with DePex mounting medium was executed (BDH Prolabo). All washing steps were performed in tap and distilled water.

2.10 Hormone measurements

Blood samples (approximately 100µl) were collected at five time points of the menstruating protocol, day 0 (one day prior to the first 100ng E2 injections), day 3 (the day of the last 100ng E2 injections), day 7 (the day of the first 5ng E2 injections), day 9 (the day of decidualization) and day 13 (immediately before the animals were sacrificed) (Figure 1). Blood sampling at day 0, 3, 7 and 9 was performed from the *vena* submandibularis. At day 13, blood samples were obtained through cardiac puncture. The collected blood was left to coagulate at room temperature for 30 minutes. Hereafter, the samples were centrifuged at 3000rpm for 10 minutes and the serum was separated from the residual material. Centrifugation was repeated to ensure that only serum was collected. Enzyme-linked immune sorbent assays (ELISAs) were conducted to measure the progesterone and estrogen levels at the different time points. Progesterone was analyzed using a progesterone rat/mouse ELISA kit (Mediatech, Kiel-Wellsee, Germany), whereas the estrogen concentrations were evaluated using a Mouse/Rat Estradiol ELISA kit (Calbiotech, Spring Valley, USA). Each of the used kits required 25µl of the serum sample and the provided standards. All steps were performed at room temperature. Hormonal levels could only be measured in singular due to a restricted amount of sample. Therefore, significant outliers were excluded (calculation of significant outliers in section 4).

2.10.1 Progesterone measurements

Serum samples from day 9 and day 13 were analyzed. In short, six standards and sixty-eight samples were added to the appropriate wells, followed by the addition of 50µl incubator buffer. After adding 100µl enzyme conjugate, the plate was incubated for one hour on a microplate mixer. Hereafter, wells were washed four times and 200µl substrate solution was added. After 30 minute incubation without shaking in the dark, 50µl of the stop solution was added. Subsequently the absorbance was measured at 450nm using a Multiskan* FC Microplate Photometer (Thermo Scientific – Thermo fisher scientific, Walldorf, Germany) and fit using a 4 parameter logistic curve and linear-linear graph paper.

2.10.2 Estrogen measurements

Serum samples from day 0, 3, 7, 9 and 13 were measured. From day 0, a selection of eight samples (two from every delivery group) was analyzed. From the remaining days, samples from all animals were included. Briefly, six standards and 136 samples were loaded and 100µl enzyme conjugate was added. Subsequently, the plate was mixed and incubated for 120 minutes. Washing of the wells was performed three times and 100µl substrate solution was added before incubating for 30 minutes. To stop the reaction, 50µl stop solution was added to each well and the absorbance

was read at 450nm using a Multiskan* FC Microplate Photometer and fit using a 4 parameter logistic curve and linear-linear graph paper.

2 Immunohistochemistry

Paraffin-embedded mouse peritoneal and skin tissue was cut into serial sections of 4µm on the HM 340 E Rotary Microtome. Visualization of the immunostaining was performed with a Zeiss Axioskop Microscope equipped with an AxioCam MRC5 and pictures were taken using Zen 2011 software.

2.2 Optimization PGP9.5 staining

PGP9.5 was stained with polyclonal rabbit anti-PGP9.5 (Dako, Glostrup, Denmark). To ensure that tissue sections would not detach from the slide during the staining, sections were preheated for 3.5 hours at 55°C before deparaffinization and rehydration. Additionally, all dilutions and rinsing steps throughout the staining protocols were performed in 0.01M tris-buffered saline (TBS) and all steps were carried out at room temperature, unless stated differently.

2.2.1 REAL detection kit

Mouse peritoneum was heat retrieved for one hour at 90°C. After Heat Induced Antigen Retrieval (HIAR), tissue sections were gradually cooled down. Slides were extensively washed and non-specific immunoglobulin binding was blocked by a one hour incubation with a block buffer containing 2% bovine serum albumin (BSA, Sigma-Aldrich), 1% non-fat dry milk (NFDM; Nestlé, Anderlecht, Belgium), 0.1% Tween (Merck, Schuchardt, Germany) and 1:30 normal goat serum (Dako). Sections were incubated overnight at 4°C with polyclonal rabbit anti-PGP9.5 (Dako; 1:500 or 1:1000). Tissue sections incubated without primary antibody were used as a negative control. Subsequently, the slides were washed and an additional blocking step was executed for 15 minutes. Antibodies were detected using the REAL Detection System, Alkaline Phosphatase/RED, Rabbit/Mouse (Dako) according to the manufacturer's instructions. In short, tissue sections were incubated with a secondary antibody for 30 minutes. After removing the secondary antibody, an alkaline phosphatase solution was added to the slides for 15 minutes. Hereafter, sections were washed and a twenty-minute incubation with the CHROM working solution was executed. Prior to mounting with glycerin jelly, slides were counterstained with Mayer hematoxylin for 15 seconds.

2.2.2 NBT/BCIP

Mouse skin and mouse peritoneum were heat retrieved at 90°C in citrate buffer (pH 6, 0.01M citrate) or tris(hydroxymethyl) aminomethane hydrochloride (Tris-HCl; pH 9, 0.01M Tris-HCl) supplemented with 1mM ethylenediaminetetraacetic acid (EDTA; Sigma-Aldrich). After one hour of HIAR, tissue sections were progressively cooled down. Slides were extensively washed and a one hour blocking step was performed using the previously described block buffer. Subsequently, sections were incubated overnight at 4°C with polyclonal rabbit anti-PGP9.5 (Dako) diluted 1:100, 1:500, 1:1000. As a negative control, tissue sections incubated without primary antibody were used. The following day, the slides were washed and additionally blocked for 15 minutes. Slides

were incubated for 30 minutes with a biotinylated swine anti-rabbit secondary antibody (Dako) diluted 1:400 and supplemented with 1:25 normal mouse serum (Dako). After washing off the secondary antibody, streptavidin conjugated alkaline phosphatase (Roche Diagnostics, Almere, The Netherlands) diluted 1:1000 was added to the slides for 30 minutes. Extensive washing was followed by incubation with nitro blue tetrazolium/5-bromo-4-chloro-3-indolyl phosphate (NBT/BCIP; Roche). The combination of NBT/BCIP reacts with alkaline phosphatase, as NBT serves as an oxidant and BCIP as a substrate for alkaline phosphatase. The NBT/BCIP reaction was assessed in time and stopped by washing the slides when sufficient staining was observed. Sections were counterstained for 30 minutes with methyl green (Dako), 2 minutes with Fast Red (Trevigen, Gaithersburg, USA) or 10 seconds with Mayer hematoxylin and mounted with glycerin jelly.

3 Pain tests

One day prior to the experiments, the lower abdomen of five mice was shaven and the animals were acclimatized to the experimental setup for one hour. Habituation of the animals to the experimental setup was needed to reduce stress during the pain tests. Temperature and mechanical sensitivity assessing tests were carried out during the day portion of the circadian cycle only (06:00-20:00h). At the day of the tests, animals were accommodated to the experimental setup for approximately 10 minutes, until cage exploration ceased. All pain tests were randomized, recorded on camera and blindly evaluated. Additionally, no other experiments were performed in the room when behavior testing occurred. Data from the experiments were obtained together with Katrien De Clercq (KU Leuven), who described the data more extensively in her master thesis.

3.2 Optimization of pain tests

Hot water tests, acetone test, von Frey hair test and running wheel test were performed 24 hours before and after a subcutaneous injection with 50 μ l CFA (Sigma-Aldrich) on each side of the lower abdomen. Parameters representative of nocifensive pain in relation to temperature sensitivity (acetone test and hot water tests) were determined after analyzing the video images. Hereafter pain tests were analyzed according to the prescribed parameters.

3.2.1 Hot water test

Polyethylene glycol 400 (PEG400; Sigma-Aldrich) was used in the hot water tests. PEG400 was chosen because it has the advantage of sticking onto the lower abdomen of the animal. Water was not used since it would easily fall off the abdomen. PEG400 was heated to 37°C, 45°C or 50°C and applied to the lower abdomen of the animal. The 37°C temperature was used as a control, under normal circumstances this temperature is perceived as innocuous by the animals. The behavior of the animals to the heat stimulus was observed during two minutes.

3.2.2 Acetone test

The animal was fixed and 50µl of acetone (Sigma-Aldrich) was applied on the lower abdomen. The subsequent behavior of the animal was assessed during two minutes.

3.2.3 Von Frey hair test

A series of von Frey hairs with logarithmically incremental stiffness (0.008, 0.02, 0.04, 0.07, 0.16, 0.4, 0.6, 1, 1.4, 2; Bioseb, Vitrolles, France) were applied to the lower abdomen of the animal. The hairs were presented with sufficient force to provoke slight bending of the hairs, while holding pressure for six seconds. A positive response was observed when the animal touched the lower abdomen or when sharply arching the back. After a positive response, a von Frey hair of lower stiffness was presented to the animal. Contrary, a von Frey hair with higher stiffness was applied when a positive response was absent. This was repeated until an array of five hairs was presented after the first positive response. The 50% response threshold (T50) was calculated from the pattern of positive and negative responses using the formula:

$$T50 = X_f + (k \times \text{mean difference})$$

where X_f = the value of the last von Frey hair used in log units; the k = the tabular value of the positive/negative response pattern as described by *Dixon* (68); and the mean difference = the mean of the differences between stimuli in log.

3.2.4 Running wheel test

Voluntary locomotive activity of the animals was assessed using the running wheel test. Seven days prior to the experiment, animals were trained by placing five mice into one running wheel cage to stimulate collaborative learning of the running wheel. One day prior to the experiments, each animal was placed separately in a running wheel cage. Running wheel cages consisted of a running wheel connected to a velocity meter, measuring the voluntary mobility of the animals. The running wheel experiments were conducted during 15 hours and the average velocity in kilometers per hour, total running length in kilometers and total running time in hours were determined.

4 Statistical analysis

Data were statistically analyzed using GraphPad Prism 5.01 software (GraphPad software Incorporated, La Jolla, USA). Results are given as mean \pm standard deviation (SD). D'Agostino normality test was used to evaluate the Gaussian distribution. The Wilcoxon matched pairs test was employed for paired data sets that did not pass normality. Additionally, non-parametric unpaired data sets were analyzed using the Kruskal-Wallis test followed by Dunn's multiple comparison test or the Mann Whitney test. Calculation of significant outliers was performed using the Grubb's test at significance level 0.01. P-values below 0.05 were considered significant (* p-value<0.05; ** p-value<0.01; *** p-value<0.001).

Results

1 Optimization of the decidualization process

This part of the study focused on the improvement of the decidualization process in the MMM and mainly aimed to determine the most effective way to obtain the most decidualized endometrial tissue. An increased yield of decidualized tissue from the MMM is needed to ensure that a minimal amount of donor animals will be used when applying the MMM in endometriosis research. Furthermore, it was contemplated that the acquisition of bicornuate decidualization would produce the highest amount of decidualized endometrium.

It was hypothesized that laparotomic or laparoscopic intrauterine oil delivery would result in 100% decidualized endometrium in both uterine horns while performing decidualization by vaginal injection would only result in bicornuate decidualization in 50% of the animals. Therefore, the effect of different intrauterine oil delivery routes on the decidualization of both uterine horns was evaluated. Characteristics of decidualization were assessed and the capability of producing bi-horned decidualization was evaluated in combination with the production of the amount of decidualized endometrium. Additionally, the hormonal concentrations were appraised both qualitatively as quantitatively and the bleeding of the animals was determined.

1.1 Uterine expansion and morphologic alterations characterized the decidualization process

To determine whether decidualization was present, both macroscopic as microscopic characteristics of the decidualization process were evaluated. Macroscopically, the size of the uterine horns was assessed. When decidualization was existent, an expansion of the uterus was observed (Figure 2A). Subsequently, the uterine expansion was further appraised by determination of the uterine weight, adjusted for the animals' body weight (relative uterine weight, as percentage of body weight), in the vaginal injection, the laparotomic injection and the laparoscopic injection group (Figure 2B). Assessment of the relative uterine weight showed a significant increase in both the laparotomic ($0.949\% \pm 0.466$; $p\text{-value} < 0.01$) as the laparoscopic injection group ($0.944\% \pm 0.6428$; $p\text{-value} < 0.05$) compared to the sham group ($0.302\% \pm 0.413$). Contrary, no significant differences were observed when comparing vaginal injections ($0.5498\% \pm 0.525$) with the sham group ($0.302\% \pm 0.413$). Furthermore, the absence of significant differences in relative uterine weight between the three delivery groups was determined.

Microscopic verification of the decidualization was performed according to the morphology of the uterus. A uterine horn without decidualization had a visible uterine lumen, a thick myometrial layer and an endometrium consisting of endometrial glands, stromal cells and epithelial cells (Figure 2C). In contrast, decidualized uterine horns were characterized by an expansion of the endometrial stromal tissue, closure of the uterus lumen and thinning of the myometrium (Figure 2D).

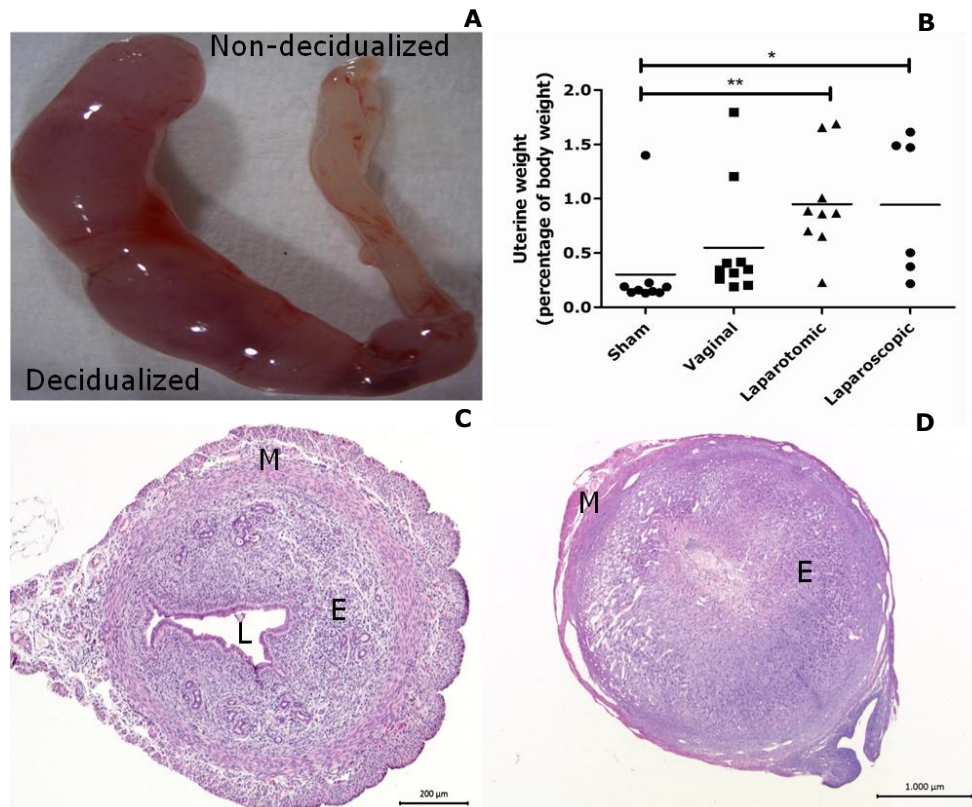


Figure 2: **Decidualization was characterized by uterine expansion and morphologic alterations.** Decidualization was induced through the delivery of intrauterine oil by means of vaginal, laparotomic or laparoscopic injections. Decidualization was assessed macroscopically by an expansion of uterine size (**A**). The uterine expansion was further evaluated in the three intrauterine oil delivery groups by determination of the uterine weight, adjusted for the body weight of the animal (**B**). Data from the uterine weight was statistically analyzed using the Kruskal-Wallis test followed by Dunn's multiple comparison test (* p-value<0.05; ** p-value<0.01; *** p-value < 0.001). Microscopic, non-decidualized horns (**C**) were distinguished from decidualized horns (**D**) by utilizing parameters such as amplification of the endometrial stromal tissue, closure of the uterine lumen and thinning of the myometrium. The scale bar of **B** describes 200µm, that of **C** 1000µm [L: uterine lumen, E: endometrium, M: myometrium].

1.2 **Bicornuate decidualization was facilitated by all three intrauterine oil delivery methods**

The effect of the delivery method of intrauterine oil on the decidualization of the uterine horns was assessed to indicate whether both uterine horns could become decidualized. To determine the success rate of the occurrence of decidualization, the presence of decidualization was only established when both macroscopic and microscopic features of the decidualization process were present.

Decidualization was absent in 88% of the animals in the sham group. In this group, one animal exhibited decidualization of both uterine horns (Figure 3). When comparing the three intrauterine oil delivery methods, it was shown that all three methods were incapable of provoking decidualization in 100% of both uterine horns. However, decidualization did occur in 70% of the animals in the vaginal injection group, 84% of the animals in the laparoscopic injection group and 88% of the animals in the laparotomic injection group. Nonetheless, the administration of intrauterine oil by all three delivery methods achieved decidualization of both uterine horns. Bicornuate decidualization was most frequently accomplished by either laparoscopic or laparotomic

injections. Within the laparoscopic and laparotomic injection groups, decidualization was always reflected in both uterine horns as the success rate of bi-horned decidualization in the laparoscopic injection group amounted to 84% and 88% of the animals in the laparotomic injection group developed bicornuate deciduas. In contrast, only 30% of the animals in the vaginal injection group obtained decidualization in both horns (Figure 3). When evaluating the effectiveness of decidualization in only one uterine horn, it was shown that vaginal injections were superior to laparoscopic and laparotomic injections. In contrast to the absence of one-horned decidualization in the laparoscopic and laparotomic injection groups, decidualization of one uterine horn occurred in 40% of the animals treated with vaginal injections (Figure 3).

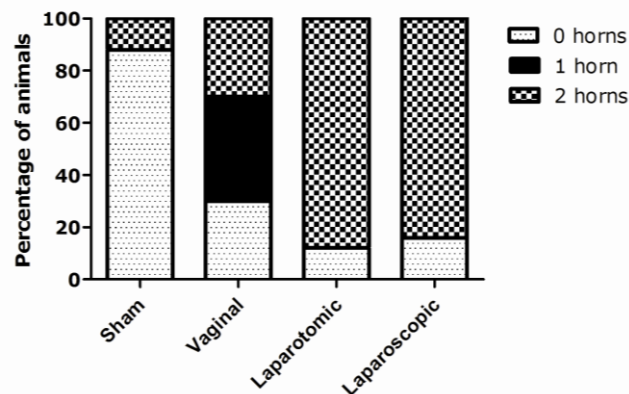


Figure 3: **Laparotomic and laparoscopic injections of intrauterine oil mainly resulted in decidualization of both uterine horns.** Decidualization was induced through the delivery of intrauterine oil by means of vaginal, laparotomic or laparoscopic injections. Decidualization was established when both macroscopic and microscopic characteristics of the decidualization process were observed. The success rate of decidualization was evaluated in relation to the number of decidualized uterine horns per group. Results of the success rate are represented as the percent of animals in the sham group (n=9), vaginal injection group (n=10), laparotomic injection group (n=9) or laparoscopic injection group (n=6) that developed either zero, one or two decidualized uterine horns.

1.3 The endometrial surface area of decidualized uteri was comparable between the three intrauterine oil delivery groups

When macroscopically assessing the decidualized uterine horns, differences in the extent of decidualization were observed. Decidualization varied between different uteri and was seen unevenly distributed across the length of the uterine horn (Figure 4A). Since this finding could denote that not every decidualized uterus generated an equivalent amount of decidualized endometrium, differences in the extent of decidualization between the intrauterine oil delivery groups were assessed and compared to the sham group. To establish the extent of decidualization, the endometrial surface area was evaluated by means of surface measurements on multiple cross-sections of both uterine horns. All uteri from the sham group were included in the measurements. In contrast, only uteri that developed a decidualized endometrium in one or two horns were measured in the three delivery groups.

A significant difference (p -value<0.05) was present between the endometrial surface area of uteri in the sham group and that of the decidualized uteri from the laparotomic and laparoscopic injection group. Additionally, in all three delivery groups the endometrial surface area was

equivalent (vaginal injections $2.227\text{mm}^2 \pm 1.187$ vs. laparotomic injections $3,091\text{mm}^2 \pm 0.678$ vs. laparoscopic injections $3.065\text{mm}^2 \pm 1.530$), as no significant differences were observed between the decidualized uteri of the three groups (Figure 4B).

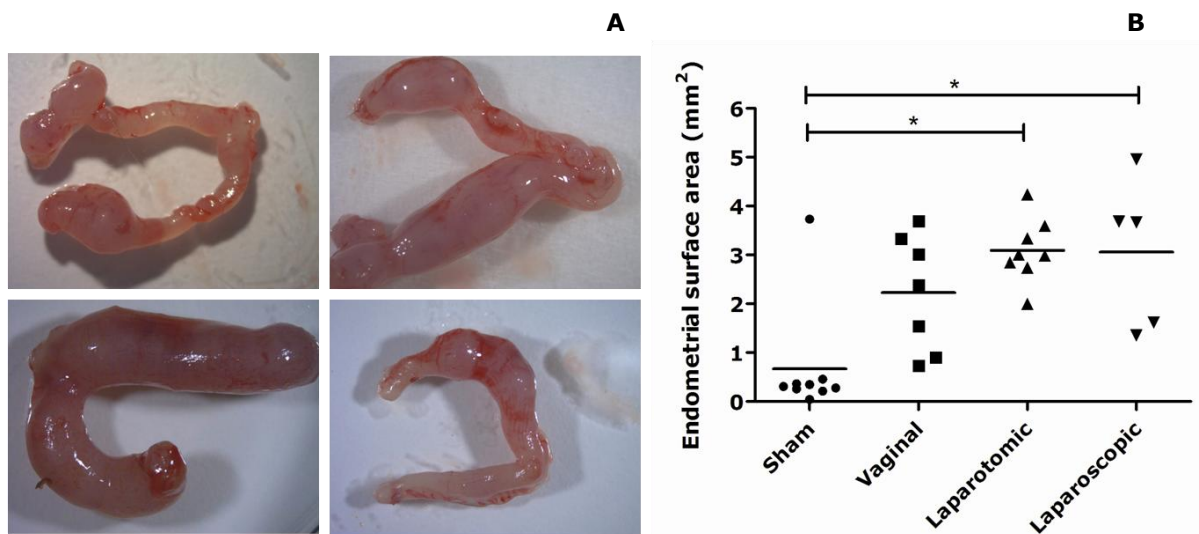


Figure 4: **Extent of uterine decidualization.** Large differences in the extent of decidualization were observed as decidualization unevenly spanned the length of the different uterine horns (**A**). To determine which intrauterine oil delivery method yielded the highest amount of decidualized endometrium, the endometrial surface area (mm^2) of decidualized uteri from the three oil delivery groups (vaginal injection group $n=7$; laparotomic injection group $n=8$; laparoscopic injection group $n=5$) were evaluated and compared with uteri from the sham group ($n=9$) (**B**). The data are represented as the endometrial surface area of every uterus and statistical analysis was performed by means of Kruskal-Wallis test followed by Dunn's multiple comparison test (* $p\text{-value}<0.05$; ** $p\text{-value}<0.01$; *** $p\text{-value}<0.001$).

1.4 Laparotomic and laparoscopic injections differed in mortality and inflammatory response

Although the relative uterine weight, the success rate and the endometrial surface area of decidualization in the laparotomic and laparoscopic intrauterine oil injection groups were similar, some differences between both techniques were observed. One discrepancy was found within the mortality of the different procedures. During the execution of both techniques, there were animals that did not survive. However, laparotomic injections lead to the death of only one animal while three animals died during the laparoscopic procedure. Additionally, when microscopically evaluating the cross-sections of decidualized uteri, side effects of the laparotomic intrauterine oil delivery method became apparent. A large influx of inflammatory cells was observed in one animal while other animals exhibited slightly inflamed decidualized tissue. In contrast, inflammation was not observed in uterine horns decidualized by means of laparoscopic injections (data not shown).

1.5 Vaginal smears monitored the hormone sensitization and the induced bleeding

Vaginal smears were conducted to evaluate both the effectiveness of the hormone sensitization as the presence of bleeding on day 13 of the menstruating protocol. Firstly, staging of the estrous cycle showed that within days after ovariectomy, all animals evolved to metestrus, a stage of low E2 concentration. Additionally, none of the ovariectomized animals entered a new cycle, which is characterized by a transition from proestrus to estrus. Results also demonstrated that all treated

animals initiated a new cycle and progressed towards the estrus stage after 100ng E2 injections. Additionally, concomitant with the implantation of the P4 pellet and the 5ng E2 injections, the animals were seen to cycle between metestrus and diestrus (Supplementary data table 1). Secondly, determination of the presence of bleeding after progesterone withdrawal showed that blood was existent in ten out of the twenty-one animals that received a decidualization stimulus. However, no delivery-group-related pattern was observed (data not shown).

1.6 E2 and P4 circulating serum concentrations

Although the vaginal cytology was indicative for the successful absorption of the administered hormones, it could not be used to assess the actual hormonal concentrations the animals were subjected to. Measurements of the E2 and P4 levels were performed by means of ELISA in serum collected at different time points. The E2 concentration was determined in samples taken from day 0, day 3, day 7, day 9 and day 13 while the P4 serum concentrations were appraised in samples collected day 9 and day 13.

1.6.1 The hormonal sensitization was reflected in the E2 and P4 serum concentrations

The E2 and P4 levels were measured to evaluate whether the desired hormonal environment was created. Results from the E2 measurements demonstrated low E2 concentrations after ovariectomy (day 0; 2.874pg/ml \pm 1.776). At day 3, after 100ng E2 injections, the E2 concentration was seen increased to 152.7pg/ml \pm 79.53. In addition this concentration was shown to be significantly higher compared to the concentrations measured on the remainder of days (p-value<0.001). No significant differences were observed in the E2 concentration after 5ng E2 injections at day 9 (11.4pg/ml \pm 6.216) compared to day 7 (7.513pg/ml \pm 5.285) or day 13 (6.315pg/ml \pm 2.275) (Figure 5A). Concerning progesterone, a concentration of 22ng/ml \pm 8.074 was present after three days of pellet implantation at day 9. Furthermore, a significant decrease (p-value<0.001) was observed after removal of the progesterone pellet at day 13 (5.867ng/ml \pm 3.214; Figure 5B).

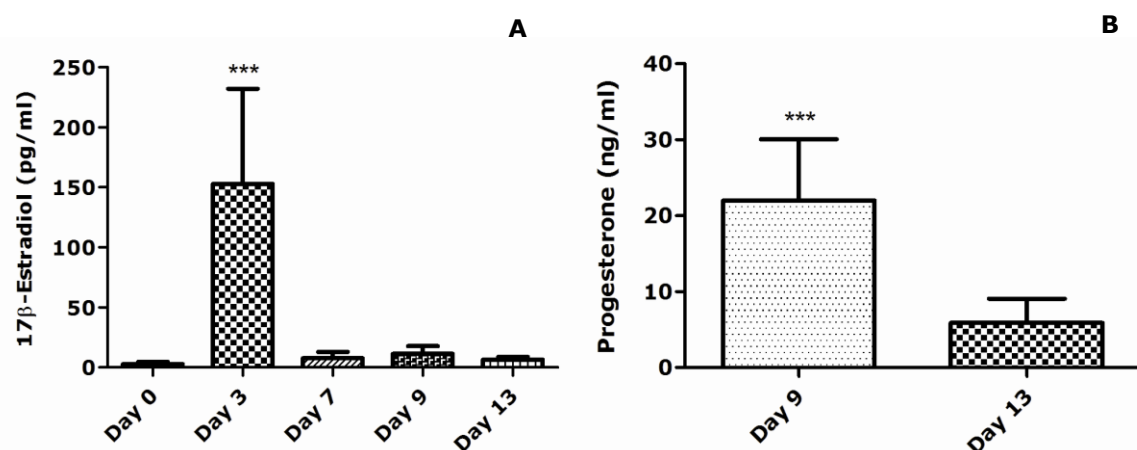


Figure 5: **Effect of hormone sensitization on the serum concentration of E2 and P4.** Ovariectomized animals underwent hormone sensitization by means of E2 injections (100ng and 5ng) and a progesterone pellet. Blood samples were taken on day 0 (one day prior to the first 100ng E2 injections), day 3 (the day of the last 100ng E2 injections), day 7 (the day of the first 5ng E2 injections), day 9 (the day of decidualization) and day 13 (immediately before the animals were sacrificed). E2 (**A**) and P4 (**B**) serum concentrations were determined by means of ELISA. Data are represented as mean \pm standard deviation and were statistically analyzed using Kruskal-Wallis test followed by Dunn's multiple comparison test (E2 data) or Mann-Whitney test (P4 measurements) (* p-value<0.05; ** p-value<0.01; *** p-value<0.001) [E2: 17β-estradiol, P4: progesterone].

1.6.2 No differences in E2 or P4 serum concentrations were observed in animals that developed or failed to develop a decidualized endometrium

Hormonal levels were also analyzed to determine whether aberrations in the concentrations of E2 and P4 could form the basis for failed decidualization. To this end, E2 and P4 serum concentrations were compared between animals receiving a decidualization stimulus that did or did not develop a decidualized uterus. No significant differences in both E2 as P4 concentrations between non-decidualized and decidualized uteri were present. However, a trend (p -value=0.0592) towards decreasing concentrations of E2 serum levels at day 3 of the menstruating protocol was observed in the animals that developed a decidualized endometrium (Figure 6). Additionally, assessment of the hormonal concentrations and the success rate of one or two decidualized uterine horns showed that no correlation exist between the serum concentrations of E2 and P4 and the acquisition of one or two decidualized horns (data not shown).

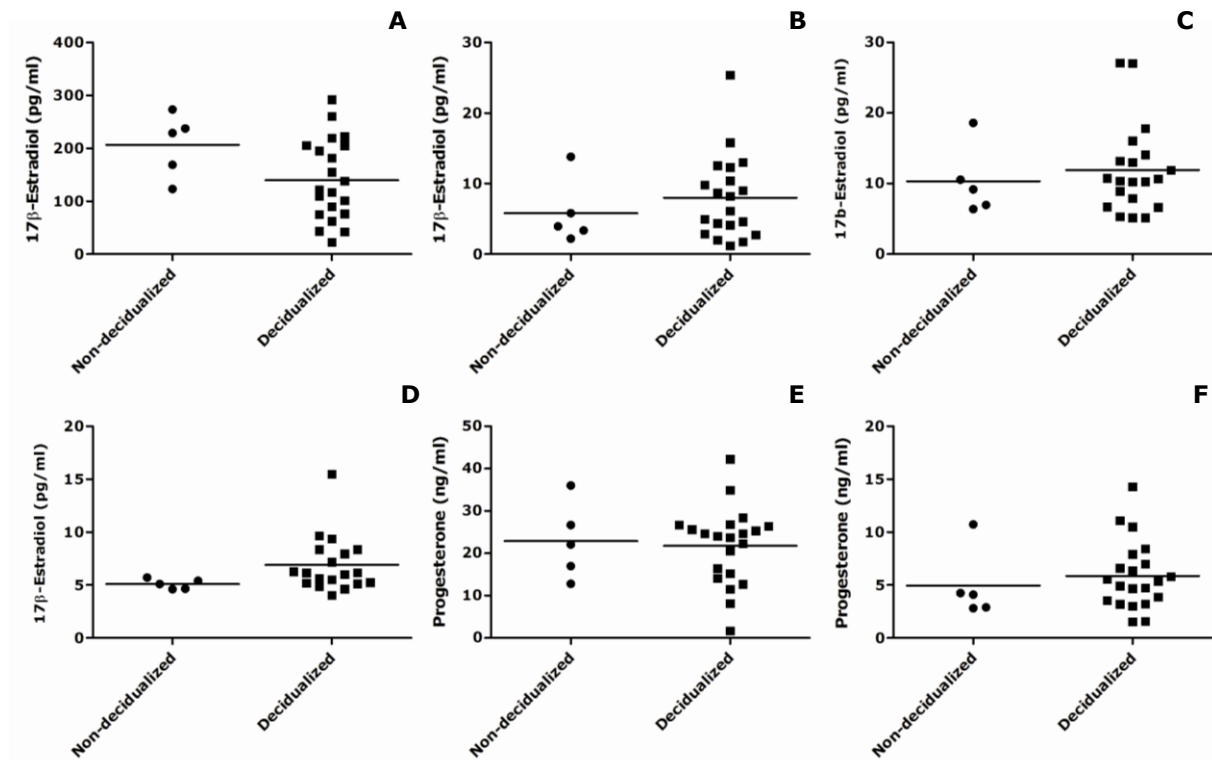


Figure 6: **No differences in hormonal concentrations were observed between animals that received a decidualization stimulus and did or did not develop a decidualized uterus.** Serum concentrations of E2 and P4 were measured by means of ELISA. Subsequently a comparison was made between animals from the three intrauterine oil delivery groups that developed (decidualized) or failed to develop a decidualized uterus (non-decidualized). E2 concentrations of day 3 (**A**; the day of the last 100ng E2 injections), day 7 (**B**; the day of the first 5ng E2 injections), day 9 (**C**; the day of decidualization) and day 13 (**D**; immediately before the animals were sacrificed) were compared. P4 measurements were performed on serum samples from day 9 (**E**) and day 13 (**F**). Statistical analysis was done using the Mann-Whitney test [E2: 17 β -estradiol, P4: progesterone].

2 Optimization of the staining protocol for PGP9.5

The importance of nerve fibers in the pathogenesis of endometriosis is exemplified by the role of neurogenesis in the development of endometriotic lesions and neuroangiogenesis in endometriosis-associated pain. To evaluate the presence of nerve fibers in endometriotic lesions, immunohistochemical stainings can be used. One marker commonly employed to evaluate the

presence of neurons is PGP9.5, a neuron specific protein that is expressed in all types of neurons. In order to obtain the optimal staining protocol for PGP9.5, the outcome of the immunostainings was evaluated using, different chromogens, antibody concentrations and HIAR methods. Additionally, peritoneal and skin tissue was used to evaluate the optimal positive control tissue.

2.1 Non-specific signal accompanied the visualization of PGP9.5 with the REAL Detection kit

Immunohistochemical detection of PGP9.5 in mouse tissue was performed by adapting a staining protocol from *Bokor et al* (69) and researchers from Edinburgh University (unpublished data). Mouse peritoneum was incubated with antibodies directed against PGP9.5 diluted 1:500 and 1:1000, followed by visualization of the antibody was using the REAL Detection kit. The presence of non-specific background staining was seen in both sections stained with the primary antibody in 1:500 (Figure 7A) and 1:1000 dilution (Figure 7B). Additionally, background staining of the tissue sections was visible as shown by the presence of signal on the negative control (no primary antibody) (Figure 7C and D). Hence, these results justified the need for additional optimization of the staining protocol for PGP9.5.

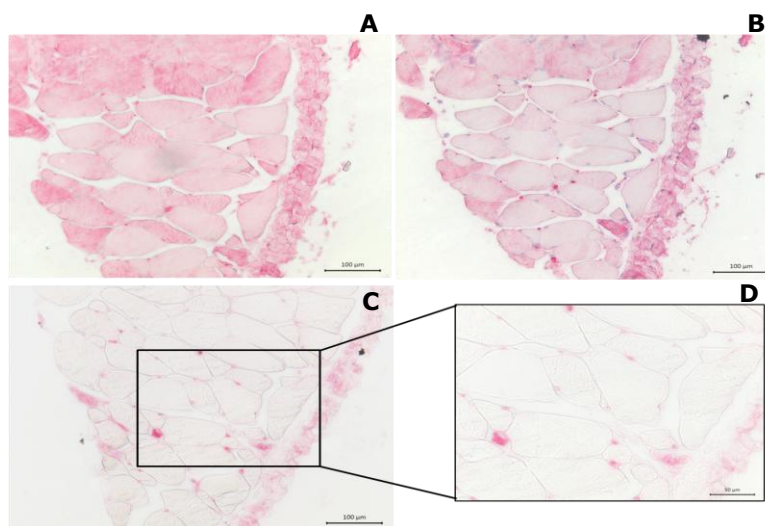


Figure 7: **Non-specific signal was observed when PGP9.5 was visualized using the REAL Detection kit.** Mouse peritoneum was incubated with rabbit anti-PGP9.5 diluted 1:500 (**A**) or 1:1000 (**B**) and detection of the antibody was performed using the REAL Detection kit. Slides that were not incubated with the primary antibody were used as negative control (**C**, **D**). Scale bars of **A**, **B**, and **C** are 100µm, that of **D** is 50µm [PGP9.5: protein gene product 9.5].

2.2 PGP9.5 visualization using the chromogenic pair NBT/BCIP

In order to improve the staining protocol for PGP9.5, optimization was performed by determining the effect of a different chromogenic pair (NBT/BCIP), different HIAR methods and an additional primary antibody dilution on the outcome of the immunohistochemical staining. As opposed to the previous staining protocol, mouse skin was included. Similarly to the use of human skin as a positive control for PGP9.5 stainings in human samples, mouse skin could function as a positive control when staining for PGP9.5 in mouse samples.

2.2.1 Tris-HCl supplemented with EDTA heat retrieval produced excessive staining

Mouse skin and peritoneum were heat retrieved in Tris-HCl supplemented with EDTA. Hereafter, incubation with the primary antibody diluted 1:100, 1:500 and 1:1000 was performed followed by visualization of the antibody using the chromogenic pair NBT/BCIP. The chromogenic reaction was

stopped when sufficient color reaction was observed. Results showed that both peritoneal as skin tissue sections heat retrieved with Tris-HCl supplemented with EDTA exhibited a tremendous amount of non-specific staining. Severe non-specific staining impeded the identification of nervous tissue in both peritoneal as skin sections when using antibody dilutions of 1:100 and 1:500 (data not shown). In peritoneal tissue, large nerve bundles could weakly be distinguished from the non-specific staining at a primary antibody dilution of 1:1000. However, small nerve fibers were not observed (Figure 8A). Additionally, an even higher amount of non-specific staining was observed in skin tissue applying a primary antibody dilution of 1:1000, making it impossible to detect nervous tissue (Figure 8B).

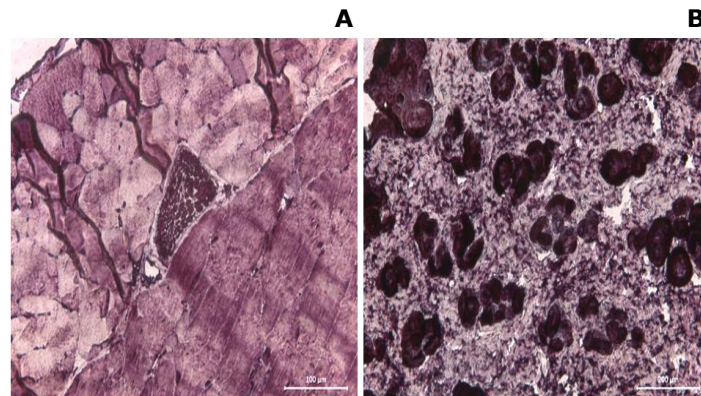


Figure 8: **Non-specific staining was observed when heat retrieving with Tris-HCl supplemented with EDTA.** Mouse peritoneum (**A**) and skin (**B**) were heat retrieved using Tris-HCl supplemented with 1mM EDTA. Incubation with rabbit anti-PGP9.5 primary antibody diluted 1:1000 was performed. Hereafter, visualization of the staining was accomplished using the chromogenic pair NBT/BCIP and a counterstaining with methyl green was performed. Scale bar of **A** represents 100µm, that of **B** 200µm [PGP9.5: protein gene product 9.5, EDTA: ethylenediaminetetraacetic acid, Tris-HCl: tris(hydroxymethyl) aminomethane hydrochloride, NBT/BCIP: nitro blue tetrazolium/5-bromo-4-chloro-3-indolyl phosphate].

2.2.2 Citrate heat retrieval and a 1:1000 antibody dilution best detected PGP9.5

HIAR was performed on mouse skin and peritoneum using citrate buffer. Hereafter the tissues were incubated with a primary antibody diluted 1:100, 1:500 and 1:1000, followed by visualization of the antibody using NBT/BCIP. The chromogenic reaction was stopped when sufficient color reaction was observed. Contrary to Tris-HCl-related HIAR, heat retrieval with citrate buffer resulted in a lower amount of non-specific background staining. In the peritoneum, nerve bundles were weakly differentiated from the non-specific staining when a 1:100 antibody dilution was used (Figure 9A). A better signal to noise ratio was observed when PGP9.5 was stained with the primary antibody diluted 1:500. However, non-specific signal was still pronouncedly present (Figure 9B). The nerve bundles were best visualized using an antibody dilution of 1:1000, as the least amount of non-specific staining was associated with this dilution of the antibody (Figure 9E). In mouse skin, diluting the primary antibody 100 or 500 times resulted in excessive staining (Figure 9C and D). Within these concentrations, nerve fibers could not be distinguished from non-specific staining. When using a primary antibody concentration of 1:1000, nerve fibers were observed in the extracellular matrix between the dermal glands and dermal papillae (arrows; Figure 9G). However, a considerable amount of background signal was still present. The absence of staining signal on both the negative control of the peritoneum as the skin section illustrated that the secondary antibody did not bind non-specifically to the tissue (Figure 9F and H).

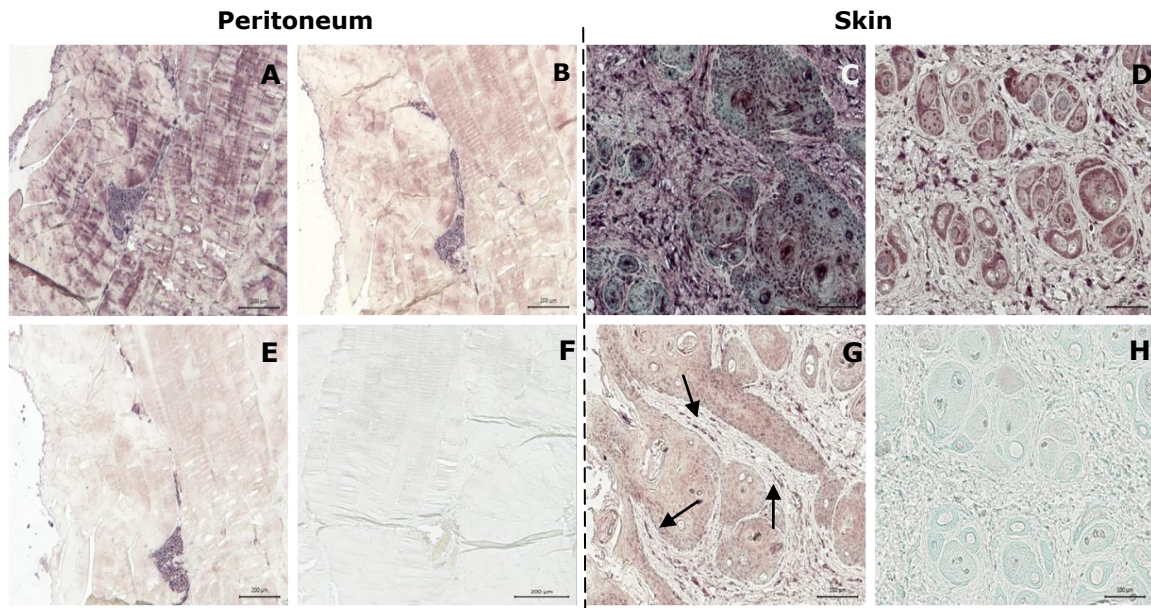


Figure 9: **Diluting the primary antibody 1000 times best detected PGP9.5 after citrate heat retrieval.** Mouse peritoneum (**A, B, E, F**) and skin (**C, D, G, H**) were heat retrieved using citrate buffer and incubated with a primary antibody directed against PGP9.5 diluted 1:100 (**A, C**), 1:500 (**B, D**) and 1:1000 (**E, G**). As a negative control, tissue sections without primary antibody incubation were used (**F, H**). Visualization of the antibody staining was achieved using the chromogenic pair NBT/BCIP and subsequently a counterstaining with methyl green was performed for 30 minutes. Arrows are indicative of nerve fibers and scale bars of the peritoneal sections represent 200 μ m, those of the skin sections 100 μ m [PGP9.5: protein gene product 9.5, NBT/BCIP: nitro blue tetrazolium/5-bromo-4-chloro-3-indolyl phosphate].

2.2.3 Fast Red or hematoxylin counterstaining decreased the contrast with the NBT/BCIP chromogenic reaction

PGP9.5-positive nerve fibers could be visualized after HIAR in citrate buffer, a primary antibody dilution of 1:1000, and visualization with the chromogenic pair NBT/BCIP; nevertheless, the staining protocol still exhibited some imperfections. As methyl green did not clearly display the structure of the tissues, further optimization steps were taken to improve the counterstaining. Because the PGP9.5 staining was the clearest in mouse peritoneum, the outcome of the Nuclear Fast Red and Mayer hematoxylin counterstainings was assessed on this tissue. Although the structure of the tissue was more visible when applying Fast Red or hematoxylin, the contrast between the background and the PGP9.5 staining decreased drastically (Figure 10A and B).

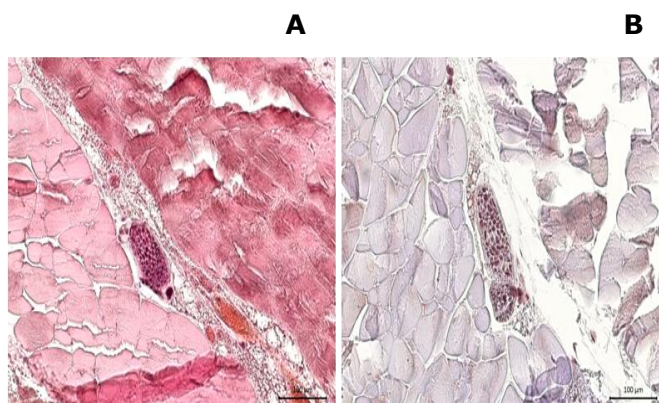


Figure 10: **A decrease in contrast with the NBT/BCIP chromogenic reaction accompanied the counterstaining with either Fast Red or hematoxylin.** Mouse peritoneum was heat retrieved in citrate buffer and incubated with a rabbit anti-PGP9.5 antibody diluted 1:1000. Visualization was performed using the chromogenic pair NBT/BCIP and counterstaining was performed using Fast Red (2 minutes; **A**) or Mayer hematoxylin (10 seconds; **B**) Scale bars represent 100 μ m. [PGP9.5: protein gene product 9.5, NBT/BCIP: nitro blue tetrazolium/5-bromo-4-chloro-3-indolyl phosphate].

3. Influence of CFA-induced abdominal pain on the nocifensive behavior of animals

Pain frequently accompanies endometriosis; however, much is still unknown about the underlying mechanisms of pain. Although pain in endometriosis could be evaluated in rodent models, it had never been examined with the array of tests used in this study. Therefore, characterization of potential changes in nocifensive behavior was performed. The locomotive activity, mechanical sensitivity and temperature sensitivity of the animals was studied in relation to a noxious inflammation, induced by subcutaneously injecting CFA. Pain tests were performed collaborating with Katrien De Clercq (KU Leuven). Since she incorporated these results in her master thesis, only the main results are summarized in this thesis.

3.1 The locomotive activity was not affected by CFA-induced abdominal pain

The effect of abdominal pain on the locomotive activity of the animals was evaluated by means of a running wheel test. Animals were placed in a running wheel cage for 15 hours and their activity was measured regarding the total distance the animals ran, the time the animals occupied running and the average velocity at which the animals ran. It was shown that CFA-induced abdominal pain did not affect the locomotive activity of the animals. No differences in the total running time, total running distance and the average speed at which the animals ran were observed when comparing data before and after CFA injection (data not shown).

3.2 A minor effect on the temperature sensitivity was observed in relation to CFA-induced abdominal pain

The acetone and hot water tests were used to assess the effects of CFA-induced abdominal pain relating to the temperature sensitivity. As these listed pain tests had never been performed before on the lower abdomen, parameters indicative of nocifensive behavior were first determined. Video images of the performed tests were analyzed and the behavior of the animals was assessed. The animals' reaching towards the application place of the stimulus was observed as a distinct behavioral characteristic. The latency towards the first response and the total time the animal spent nurturing the abdomen were also noticed as nocifensive behavior. As a consequence, nocifensive behavior in response to temperature sensitivity was analyzed according to the following parameters: the number of licks (reaching for the abdomen), time of first response (latency) and the total response time. Results showed that CFA-induced abdominal pain did not significantly alter any of the specified parameters (Figure 11).

Although no significant differences were observed, some small effects could be discerned. A minor shift in nocifensive behavior relating to CFA-induced abdominal pain within the acetone test was observed. A small increase in both the number of licks (8.4 ± 2.3 vs. 9.8 ± 3.19 ; Figure 11A) and the total response time ($29.8s \pm 7.89$ vs. $35.6s \pm 10.45$; Figure 11C) was contemplated. However, no differences with respect to the first response time were marked (Figure 11B). Additionally, the hot water test at 37°C showed a decreasing trend ($p\text{-value}=0.0625$) in first response time before and after CFA injection (Figure 11B). CFA-induced abdominal pain also weakly affected the number of licks (2.8 ± 1.30 vs. 5.6 ± 4.04 ; Figure 11A) and the total response time ($42s \pm 47.1$ vs. $59.6s \pm 46.78$; Figure 11C). A stimulus of 45°C did not influence the first response time of the animals

(Figure 11B). However, the number of licks was weakly increased (2.8 ± 3.63 vs. 4.8 ± 2.28 ; Figure 11A) and the total response time had the tendency to lengthen in response to CFA-induced abdominal pain (p -value=0.0625; Figure 11C). The nocifensive behavior regarding the total response time and first time of response were not changed by a hot stimulus of 50°C (Figure 11C and D). At 50°C, only the number of licks decreased slightly (3.2 ± 1.48 vs. 1.8 ± 1.48 ; Figure 11A).

3.3 The mechanical sensitivity of animals tended to be affected by CFA-induced abdominal pain

Since mechanical hypersensitivity is also related to the pain perception in animals, the nocifensive behavior appertaining to the mechanical sensitivity of the animals in response to CFA-induced abdominal pain was assessed by means of the von Frey hair test. CFA-induced abdominal pain eventuated into a trend (p -value=0.0625) toward decreasing the 50% threshold, a threshold at which the animals showed a positive response in 50% of the times (Figure 11D).

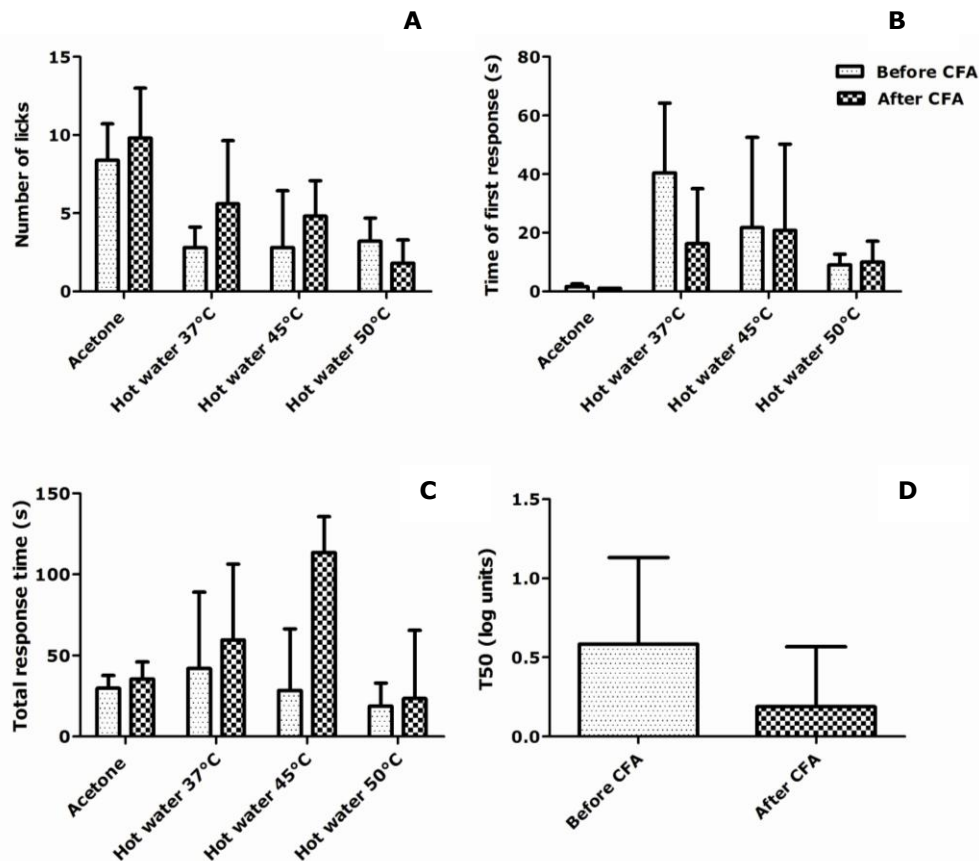


Figure 11: **CFA-induced abdominal pain had a small effect on the nocifensive behavior of animals with regard to temperature sensitive and mechanical sensitive responses.** The nocifensive effect of the mice in response to abdominal pain was evaluated. The temperature sensitivity (**A, B, C**) and mechanical sensitivity (**D**) of the animals was assessed before and after the induction of inflammatory pain by CFA. Temperature sensitivity was measured using the acetone test and the hot water test at 37°C, 45°C and 50°C and presented in relation to the number of times the animals licked the abdomen (**A**), the time at which the first response occurs (**B**) the total response time (**C**). Von Frey hair test was used to assess the effect of abdominal pain on the 50% threshold (**D**). Results are presented as average \pm SD and statistically analyzed using the Wilcoxon matched pairs test [CFA: complete Freund's adjuvant; T50: 50% threshold].

Discussion

In recent years, the development of effective diagnostic tools and treatment strategies for endometriosis has been complicated by a translational challenge. To improve this challenge, affordable preclinical models that closely mimic the disease need to be developed, thoroughly characterized and validated. In this context, the current study implemented several highly needed optimization steps for the characterization and validation of the MMM to use this model in endometriosis research.

The first aim of this study comprised the optimization of the decidualization process of the MMM. The optimal delivery method for the intrauterine oil injection had never been evaluated. Additionally, the majority of the present studies induced decidualization into one uterine horn, retaining the other horn as an internal control (57, 61-63, 70). Yet, our goal was to achieve the decidualization of both uterine horns in order to introduce a reduction in the number of donor animals for the MMM in endometriosis setting. To determine which method yielded the highest amount of decidualized tissue, the intrauterine delivery of oil by means of vaginal, laparotomic or laparoscopic injections was evaluated. It was hypothesized that laparotomic or laparoscopic intrauterine oil delivery would result in 100% bicornuate decidualized endometrium in both uterine horns while performing decidualization by vaginal injection would only result in the formation of bicornuate deciduas in 50% of the animals.

Results indicated that decidualization was present in 70% of the animals in the vaginal injection group, 84% of the animals in the laparoscopic injection group and 88% of animals in the laparotomic injection group. In the laparotomic and laparoscopic injection groups, decidualization occurred less frequent then contemplated. Nevertheless, the high decidualization percentages displayed that 100% decidualization might not be unachievable. Furthermore, compared to other groups, the success rate of decidualization was high as researchers from Edinburgh University only achieved decidualization in 50% of the animals by means of vaginal injections (unpublished data) and *Brasted et al* indicated failed decidualization in 30% of the animals that received intrauterine oil by means of laparotomic injections (61). Nevertheless, these groups all retained one uterine horn as internal control. Moreover, no research group had ever attempted the introduction of intrauterine oil by means of laparoscopic injections. Therefore the comparison between literature and the results obtained in this study concerning bicornuate decidualization was not possible. Nevertheless, in this study, it was shown that all three groups facilitated decidualization of both uterine horns. In addition, when decidualization did occur, laparotomic and laparoscopic injections always resulted in bi-horned decidualization.

The decidualization process was determined by both macroscopic as microscopic features. The significant increase in relative uterine weight in the laparotomic (p -value <0.01) and laparoscopic (p -value <0.05) injection group not only confirmed the macroscopically visible expansion of decidualized uterine horns, it also described the high success rates of decidualization in the laparotomic and laparoscopic injection groups. Additionally, although decidualization frequently occurred, macroscopically, in most of the decidualized uterine horns, decidualization unevenly

spanned the length of the horn. Complete decidualization was occasionally discerned, albeit that often the uterine horn only exhibited decidualization in one small area. To determine which delivery method yielded the highest amount of decidualized tissue, measurements of the endometrial surface area of horns from decidualized uteri were performed. It was shown that decidualized uteri from the laparoscopic and laparotomic injection group contained significantly more endometrial tissue compared to uteri from the sham group (p -value <0.05). Furthermore, the three applied techniques were determined equally capable of causing decidualization as represented by the conformity in endometrial surface area (surface area vaginal injections $2.227\text{mm}^2 \pm 1.187$ vs. laparotomic injections $3.091\text{mm}^2 \pm 0.678$ vs. laparoscopic injections $3.065\text{mm}^2 \pm 1.530$). Differences in the extent of decidualization were also noticed by *Brasted et al* who reported variability in decidualization as mice failed to develop a decidualized endometrium or showed retardation in decidualization. They minimized the differences by extending the decidualization process to 49 hours, which showed less variability than when decidualization was only given 24 or 36 hours (61). In this study, animals were sacrificed five days after the induction of decidualization by oil injection. However, as the induction of the decidualization stimulus seized a whole day, differences in the extent of decidualization could be attributed to a difference in incubation time of decidualization.

The combination of the results from the relative uterine weight, the success rate and those from the assessment of the endometrial surface area displayed no differences between both laparoscopic and laparotomic injections. Therefore, to determine which of those delivery methods should be used in further experiments, other parameters were applied. On the one hand, it was shown that one animal died during laparotomic injections while three animals died during laparoscopy. During laparotomy, the animal died due to internal bleeding while during laparoscopy the animals' death was owing to intubation difficulties. Nonetheless, within both techniques the amount of dead animals could be reduced by properly mastering the surgical procedures. On the other hand, immune cell infiltration and adhesion formation were observed after laparotomy and not after laparoscopy. This was likely caused by the induction of new wounds in both the skin and the peritoneum in order to reach the uterus. Since it is very important to implant viable donor tissue into the peritoneal cavity of recipient mice when implementing the MMM in endometriosis research, it was decided that laparoscopy is the most favorable method to perform intrauterine oil injections.

During the development of the MMM, *Finn et al* defined three requirements to induce menstrual-like changes of the uterus in animals that normally do not menstruate. These requirements indicated that (i) the endometrium of ovariectomized animals should be hormonally sensitized with estrogen and progesterone, (ii) a stimulus is needed to evoke decidualization, and (iii) a drop in progesterone is required to induce endometrial breakdown (60). Since it was indicated that a decidualization stimulus is always needed, the atypical finding of a decidualized endometrium in the sham group could be attributed to the injection of PBS during the vaginal smears. Furthermore, although laparoscopic injections were designated as the method of choice to induce decidualization, the outcome of the decidualization process was not yet optimal. Therefore, derived from *Finn's* requirements, two parameters could be responsible for the absence of decidualization in some animals: the hormone levels or the decidualization stimulus. Throughout the menstruating protocol,

preliminary results on the effectiveness of the hormone sensitization were obtained by staging the estrous cycle of the animals through the acquisition of vaginal smears. Assessment of the vaginal cytology indicated that ovariectomy was successful since all days evolved to a stage of low E2 concentration after ovariectomy. Furthermore, the successful absorption of 100ng E2 injections was established as the estrous cycle of all animals was seen entering a new cycle. Although the effect of the 100ng injection was evident, the combined effect of the progesterone pellet and 5ng E2 injections was less obvious. The animals cycled between metestrus and diestrus; however, no distinct stage was observed as characteristic for the progesterone pellet in combination with 5ng E2 injections.

Yet, as the vaginal smears merely qualitatively showed that the hormone sensitization succeeded, the serum concentrations of E2 and P4 were evaluated to establish quantitative results. It was shown that the course of the hormone sensitization, as defined by the E2 and P4 measurements, confirmed the results from the vaginal smear. Firstly, low E2 concentrations at day 0 ($2.874\text{pg/ml} \pm 1.776$) confirmed a successful ovariectomy. Furthermore, a significant increase ($p\text{-value} < 0.001$) from $2.874\text{pg/ml} \pm 1.776$ to $152.7\text{pg/ml} \pm 79.53$ at day 3 indeed showed that 100ng E2 injections were successful. Finally, the absence of a distinct characteristic for 5ng E2 injections was explained as low E2 concentrations were present at day 9 ($11.40\text{pg/ml} \pm 6.216$), however, at this time point, higher concentrations of P4 are observed ($22\text{ng/ml} \pm 8.074$). Accordingly, the estrous cycle stage leaned towards diestrus, a stage of high progesterone concentration. Results also indicated a rapid decline in progesterone levels after progesterone withdrawal ($p\text{-value} < 0.001$). To our knowledge, the E2 levels have never been studied before in this MMM. Therefore, our results cannot be compared to other studies. In contrast, progesterone levels have been studied. *Xu et al* demonstrated progesterone levels in the range of 41–52ng/ml three days after pellet implantation (62). Additionally, *Brasted et al* marked a significant decrease in progesterone concentration after pellet removal. They showed that the progesterone concentration declined from 57ng/ml to 2ng/ml after 12 hours (61). A significant decrease ($p\text{-value} < 0.001$) was also observed after pellet removal in this study. However, contrary to previous studies, our results indicated lower progesterone concentrations at day 9 ($22\text{ng/ml} \pm 8.074$). This finding could be caused by the properties of the progesterone pellet. Differences in the quantity of progesterone in the silastic tubing could result in disparate diffusion rates and may lead to aberrant hormonal concentrations. Although some differences compared to literature were established, E2 and P4 measurements showed that the fluctuations in hormones, as seen in the human reproductive cycle (Supplementary data figure 2), were correctly mimicked.

Next, potential aberrations in hormone environment of animals from the delivery groups that did or did not acquire a decidualized endometrium were examined. Results indicated no significant differences between non-decidualized and decidualized uteri from animals that received a decidualization stimulus. Merely a decreasing trend ($p\text{-value} = 0.0592$) in animals developing a decidualized endometrium was observed in E2 concentration at day 3. This trend could possibly be explained by the high variance (concentration range: $22.51\text{pg/ml} - 292.2\text{pg/ml}$) in hormonal concentrations at this time point and the low amount of non-decidualized uteri ($n=5$) for comparison. However, the observed trend might also have biologic implications. E2 is known to

stimulate the proliferation of endometrial tissue (57). Therefore, aberrations in the E2 concentrations could facilitate differences in endometrial proliferation and may have an effect on the subsequent decidualization. Nevertheless, this explanation cannot be ascertained as literature lacks the evaluation of the E2 levels in relation to decidualization. Differences in hormonal milieu between animals that developed one or two decidualized uterine horns were not observed. The absence of significant differences indicated that the involvement of hormones in the failure of decidualization is probably very limited. As the circulating serum concentrations of E2 and P4 were not determined a relevant factor which could explain the differences in success rate of decidualization, failing of decidualization could be attributed to the decidualization stimulus itself. Therefore, the success rate could probably be improved by altering the execution of the decidualization stimulus. *Rudolph et al* reported bicornuate decidualization in 80% of the animals by means of vaginal injections after applying 100 μ l sesame oil to induce decidualization. However, this study was performed in a MMM utilizing pseudo-pregnant mice (56). For this reason, a study examining the effect of the injection of 100 μ l on bicornuate decidualization in our model should be executed.

The most important advantage of the employment of the MMM in endometriosis research encompasses the transplantation of decidualized premenstrual or early menstrual endometrium into the peritoneal cavity of recipient mice to mimic the event of retrograde menstruation. Therefore, bleeding of the animals was assessed to determine whether decidualized/menstrual endometrium was created. Five hours after progesterone withdrawal, ten out of twenty-one animals that received a decidualization stimulus and developed a decidualized endometrium exhibited visual bleeding in the vaginal smear. Previous studies denounced different time points of the bleeding initiation. *Brasted et al* showed the occurrence of bleeding 12-16 hours after progesterone withdrawal, while *Menning et al* demonstrated bleeding 24 hours after progesterone withdrawal (57, 61). In addition, the drop in progesterone level has been correlated to the bleeding and the progesterone withdrawal has been ascertained as a causative factor for decidua breakdown (60, 62, 70). For this reason, the rapid disintegration of the decidualized tissue in this study could be related to the progesterone concentration (22ng/ml \pm 8.074). It is postulated that, due to this low concentration, compared to findings in literature, the progesterone level needed to induce bleeding was quickly reached. Since merely 48% of the animals with a decidualized endometrium exhibited signs of bleeding, the acquisition of menstrual endometrium might be aided by allowing a longer time for disintegration. To facilitate this, the time between the P4 pellet removal and the animal's sacrifice could be extended. However, it must be kept in mind that apoptosis and an influx of leukocytes accompanies the development of menstrual endometrium in the MMM (57, 61, 62). Theoretically, these processes might render the quality of an advanced state of disintegrated menstrual endometrial tissue too poor for implantation in recipient mice. However, in the baboon model for endometriosis, it has been shown that induction of endometriosis can be induced more successfully after intrapelvic injection of menstrual endometrium when compared to endometrium obtained during the follicular or luteal phase of the cycle (71). Therefore, in future research, the optimal dose and duration of progesterone exposure, and the optimal time interval after progesterone withdrawal needs to be evaluated, to ensure that viable decidualized early menstrual endometrial tissue can be used for injection into recipient mice.

Summarized, these results showed that laparoscopic and laparotomic injections are desired to yield a high amount of decidualized tissue. When implementing the side effects of each technique, laparoscopy was designated as the most optimal method for intrauterine oil injection. Furthermore, it was shown that the contemplated hormonal environment was created and that E2 and P4 serum concentrations probably did not contribute to failing of the decidualization. However, the current results also indicated that the decidualization process can still be improved.

In a second aim, this study assessed the optimal staining protocol for the visualization of PGP9.5. Although the expansion of endometriosis-associated neural systems is known to be important in endometriosis, the time dependent emergence of nerve fibers has not yet been studied (20, 37). For that reason, neurogenesis or neuroangiogenesis need to be evaluated in a time dependent manner utilizing the MMM in endometriosis. This will be achieved by evaluating the presence of nerve fibers at multiple time points of the lesion development through immunohistochemical staining of PGP9.5, a pan neuronal marker (72). However before visualization of PGP9.5 in endometriotic lesions could take place, optimization was needed.

The first staining protocol applied the REAL Detection kit to visualize the rabbit anti-PGP9.5 antibody. Results indicated the presence of background staining on the negative control. Background staining was thought to be ascribed to endogenous biotin, considering a biotinylated antibody was used. However, the interference of endogenous biotin was excluded as no additional blocking steps were added in consecutive stainings, yet the background staining was no longer observed. Therefore, the cause of the background staining may be owing to the type of chromogen used in the REAL detection kit. Yet, this could not be ascertained since the exact composition of the substances in the kit is unknown.

To improve the staining protocol, a new protocol containing a different chromogenic pair (NBT/BCIP) was composed. Two types of HIAR methods and multiple primary antibody dilutions were evaluated within this protocol. Furthermore, mouse skin was added to assess its quality as a positive control. Our results displayed that heat retrieval with Tris-HCl supplemented with EDTA resulted in excessive staining of the mouse peritoneum and skin throughout all the antibody concentrations. Accordingly, differences between the different antibody concentrations could not be distinguished. Contrary, antigen retrieval using citrate buffer resulted in less non-specific staining. In immunohistochemistry, antigen retrieval methods have become indispensable. Fixatives such as formaldehyde form inter- and intra-molecular cross-links in proteins and nucleic acids, resulting in the masking of antigens (73). HIAR is considered one of the most prevailing antigen retrieval methods and can be performed using a variety of solutions and heating devices. It has been noted that the optimal retrieval method often differs between antibodies (74). The observed divergence between both Tris-HCl supplemented with EDTA and citrate could be attributed to the difference in pH between the two buffers. *Emoto et al* assessed the effect of the pH during heat retrieval on the immunostaining of antigens. They showed that the pH has a large impact on the antigen retrieving capacity of a solution and that under basic conditions, the immunoreaction of a number of antigens was perceived the strongest (75). Therefore, the basic pH of Tris-HCl supplemented with EDTA could be the cause of the excessive staining signal for PGP9.5. Additionally, the large amount of

non-specific staining associated with Tris-HCl supplemented with EDTA antigen retrieval precluded the decision on the best antibody concentration.

A clear difference in the various antibody concentrations was observed when both mouse peritoneum and mouse skin sections were heat retrieved in citrate buffer. Within both tissues, the optimal signal-to-noise ratio was observed after diluting the primary antibody 1000 times. Peritoneal sections stained with this antibody dilution were clearly indicative of nerve bundles. Even though a high enough specificity was acquired, some degree of non-specific signal was still observed. Therefore, applying an antibody dilution of 1:1500 or even 1:2000 could be recommended to completely eliminate non-specific staining. In the skin section, nerve fibers were observed despite the high degree of non-specific staining accompanying the 1:1000 dilution. The non-specific staining could be ascribed to the affinity of the rabbit anti-PGP9.5 antibody to connective tissue and epithelial cells. As the skin sections were made in the papillary layer of the dermis that mainly consists of connective tissue and epithelium from the epidermis, non-specific staining was not unexpected. Therefore, additionally diluting the PGP9.5 antibody for skin tissue might not significantly alter the amount non-specific staining. Initially, mouse skin was thought to be a good positive control as during the evaluation of PGP9.5 in human samples, human skin frequently serves as positive control (69). However, our results indicated that the optimized staining protocol was not adequate to unmistakably detect nerve fibers in mouse skin tissue, hereby decreasing its value as a control tissue. Therefore, peritoneal tissue was denoted a better positive control for PGP9.5 staining.

Although nerve fibers could be distinguished with the optimized staining protocol, the outcome of the immunostaining was not impeccable as the counterstaining with methyl green did not clearly represent the tissue structure. To assess whether the staining protocol could be further optimized, counterstaining with Fast Red or Mayer hematoxylin on peritoneal tissue was evaluated. However, it was shown that neither Fast Red nor Mayer hematoxylin were superior to counterstaining with methyl green. A decreased contrast between the NBT/BCIP chromogenic reaction and the background staining with Fast Red or Mayer hematoxylin was observed. In literature, Fast Red and Mayer hematoxylin are commonly used in combination with NBT/BCIP (76). However, we were not able to obtain nice results with these counterstaining methods. Both counterstaining solutions produced a purplish color reaction even though a red and light blue color was anticipated. The aberrant outcome might be due to the nature of the counterstaining solutions. It has been noted that ready-made nuclear Fast Red solutions (as used in this thesis) are inferior to self-made solutions. Additionally, the prolonged use of the Mayer hematoxylin solution might also influence the outcome of the counterstaining. The more the solution is used, the more diluted it becomes, altering the staining ability of the solution. Due to the poor outcome of other counterstaining solutions, counterstaining with methyl green was opted for considering that a good contrast between background and immunostaining was more important than the visualization of the tissue itself. However, the methyl green counterstaining could possibly be improved by incubating the solution longer e.g. for one hour.

In conclusion, the results of the optimization of the staining protocol for PGP9.5 signified that nerve fibers could best be detected in peritoneal tissue after citrate HIAR, in combination with primary antibody dilution of 1:1000, visualization with the chromogenic pair NBT/BCIP and counterstaining with methyl green.

Lastly, this study aimed to evaluate different aspects of the nocifensive behavior of animals in response to abdominal pain to give an indication of this behavior towards endometriosis-associated pain. To date, the exact etiology of endometriosis-associated pain remains unknown (4). To increase this knowledge, pain can be evaluated in animal models of endometriosis. Nevertheless, currently there is a lack of validated pain tests for animal models of endometriosis. Therefore, the locomotive activity, mechanical sensitivity and temperature sensitivity was assessed before and after the injection of CFA in the lower abdomen using the running wheel test, von Frey hair test, acetone test and hot water tests, respectively. Throughout the set of different tests, no significant findings were observed. However, small alterations in nocifensive behavior could be observed within some of the applied tests.

Results indicated no change in the locomotive activity of the animals subjected to CFA-related abdominal pain. The lack of differences in response to the CFA-injection might indicate that the inflammation in the lower abdomen was not sufficient to induce an altered behavior of the animals with regard to their locomotive activity. The explanation for the absence of an altered behavior can be found in two possibilities. Firstly, as this study comprised a pilot experiment, only a small sample size was employed. Accordingly, a bigger sample size could show potential changes in nocifensive behavior. Secondly, the unaltered nocifensive behavior of the animals might display the presence of a 'pain threshold' for the locomotive activity in response to abdominal pain. This denotes that a certain pain level must possibly be reached in order to alter the animal's behavior. When extrapolating the possibility of a 'pain threshold' for the running wheel activity to endometriosis research, it might be recommended to include the running wheel test to assess pain in endometriosis, even though our results showed no alteration in nocifensive behavior towards CFA-induced abdominal pain.

To assess the mechanical sensitivity of the animals, the von Frey hair test was used. Results illustrated a trend towards decreasing the 50% threshold after CFA injection. These findings suggest the existence of a mechanical allodynia (a painful response to a normally innocuous stimulus).

The nocifensive behavior relating to temperature sensitivity underwent some minor alterations. It was shown that CFA-induced abdominal pain only weakly changed the animals' nocifensive behavior within the acetone test. Small differences were observed in the number of licks (8.4 ± 2.3 vs. 9.8 ± 3.19) and the total response time ($29.8s \pm 7.89$ vs. $35.6s \pm 10.45$) however, no alterations were seen in the time of the first response. The lack of difference in first response time could be attributed to the rapid cooling sensation that occurred when acetone evaporated after touching the skin of the animal. Due to this intrinsic characteristic of acetone, any difference in behavior observed in the latency toward abdominal pain was excluded. Therefore, when examining

pain in animals suffering from endometriosis, the time of first response should not be taken into account in the acetone test. Within the hot water tests, trends were observed in the first response time at 37°C (p-value=0.0625) and the total response time at 45°C (p-value=0.0625). It is generally believed that under basal conditions, 37°C is not perceived as painful for the animals (77). On the one hand, before CFA induction, some response towards the application of PEG400 at 37°C was observed. Yet, these responses could not be attributed to a noxious sensation as the latency is higher than that at noxious temperatures such as 45°C and 50°C (40.4s ± 23.86 vs. 21.8s ± 30.7 and 9s ± 3.674). On the other hand, after CFA induction, the first response time at 37°C was comparable to the first response time during the application of noxious heat (45°C) (16.2s ± 18.86 vs. 20.80s ± 18.86). This indicated that the behavior of the animals after CFA induction could likely be ascribed to nociception and that the decrease in first response time after CFA induction might denote the presence of an allodynic sensation at 37°C. The trend (p-value=0.0625) towards an increase in total response time at 45°C signified the presence of a hypersensitive reaction (increased response to a painful stimulus) towards CFA-induced abdominal pain. Besides the total response time, a minor increase in number of licks was also observed (2.8 ± 3.63 vs. 4.8 ± 2.28). In line with the hypersensitive reaction that accompanied 45°C, an even bigger hypersensitive reaction was contemplated at 50°C. Nonetheless, the obtained results indicated that the animals reacted less towards 50°C after CFA-induction. Therefore, it was assumed that this kind of noxious temperature elicited a different kind of nocifensive behavior compared to lower less-noxious temperatures. The animals all exhibited a kind of post-shock freezing behavior, indicating that this might be the expressed nocifensive behavior of animals with abdominal pain at 50°C.

Although no significant findings were observed, it is believed that the applied parameters to assess the nocifensive behavior in relation to the temperature sensitivity of the animals were valid. Previous studies investigating temperature sensitivity in the hind paw of mice also used the latency of hind paw withdrawal, the duration of withdrawal and flicking, biting, and licking behavior as parameters characteristic for pain (78, 79). This showed that the behavior of the animals observed during our tests could indeed be considered as nocifensive behavior.

The novel use of the employed array of pain tests on the lower abdomen of animals impeded comparison and validation of the obtained results. Additionally, these pain tests have never been used in the setting of endometriosis, rendering the exact nocifensive behavior of animals suffering from endometriosis unknown. Therefore, the exact behavioral characteristics can only be determined in animals experiencing endometriosis-associated pain. However, it is believed that our experiments gave an adequate representation of pain in endometriosis. The finding that inflammation attributes to the development of endometriosis-associated pain, justifies the use of CFA (4, 39). Additionally, CFA-induced inflammatory pain results in allodynia and hyperalgesia two processes that are also observed in endometriosis (39, 80, 81). For these reasons, we believe that the inflammatory pain induced by CFA injection mimicked endometriosis-associated pain closely enough to assess the potential nocifensive behavior of animals related to pain in endometriosis.

Taken together, these results indicated that changes in nocifensive behavior relating to CFA-induced abdominal pain did occur, although significance was vacant. Nevertheless, all of the applied tests should be performed within an animal model of endometriosis to determine the exact effect of endometriosis-associated pain on the nocifensive behavior of animals. The greatest value of the current study lies in the denotation of parameters subject to alterations in nocifensive behavior of the animals.

Conclusion and synthesis

The first optimization step concerned the improvement of the decidualization protocol in the MMM. When implementing the MMM in preclinical endometriosis research, a high yield of decidualized tissue is desired to reduce the number of donor animals that are needed. Therefore, the main aim of this part covered the determination of the most effective method to induce bicornuate decidualization and to yield a high amount of decidualized endometrium. Laparoscopic and laparotomic injections of intrauterine oil were determined superior to induce bicornuate decidualization. Furthermore, when taking into account side effects of the injection methods, laparoscopy was designated as the most suitable decidualization method. However, to ensure complete bicornuate, further optimization steps are still needed.

The second optimization step encompassed the identification of the optimal staining protocol for PGP9.5, a pan neuronal marker. Staining for PGP9.5 is commonly used to evaluate neurogenesis, and therefore could also be used to determine the presence of neuroangiogenesis. Results indicated that the optimal staining protocol for PGP9.5 involved antigen retrieval in citrate buffer, a primary antibody dilution of 1:1000, visualization with the chromogenic pair NBT/BCIP and counterstaining with methyl green. In addition, mouse peritoneal tissue was denoted as preferable positive control tissue.

Lastly, this study assessed the characteristics for nocifensive behavior towards abdominal pain. The behavior of the animals with regard to the temperature sensitivity (hot water and acetone tests), mechanical sensitivity (von Frey hair test) and locomotive function (running wheel test) was assessed before and after a subcutaneous injection with CFA. Results showed no significant differences, however, some trends were observed.

Taken together, this study comprised different optimization steps in prospect of the standardization and subsequent validation of the MMM for endometriosis research. When standardizing and validating a model, it is very important to assess whether the model mimics the human disease. In the setting of endometriosis, this includes modeling both the etiology as the complex pathogenesis of endometriosis. The MMM has the advantage of simulating the key event of retrograde menstruation as closely as possible by implanting decidualized premenstrual or early menstrual endometrium from a donor mouse in the peritoneal cavity of a recipient mouse. To evaluate the pathogenesis of endometriosis in this model, the different aspects of the early development of endometriosis should be assessed. To effectuate this, the presence of neurogenesis, angiogenesis, lymphangiogenesis and endometriosis-associated pain during the development of endometriotic lesions need to be appraised.

In this setting the optimization steps featured in the current study were indispensable as their outcomes can be implemented in subsequent studies on the early development of endometriosis in the MMM. Some optimization steps are still needed concerning the decidualization protocol to ensure 100% decidualization and an adequate amount of decidual degeneration. These steps include the induction of decidualization by the laparoscopic injection of 100µl intrauterine oil and

the assessment of the appropriate incubation time for decidualization. In contrast, the optimization of the PGP9.5 staining and the identification of changes in nocifensive behavior of the animals towards abdominal pain can directly be used in future experiments relating to the early development of endometriosis. Therefore, the different optimization steps performed in this study form the basis for the standardization of the MMM in preclinical endometriosis research.

References

1. Giudice LC, Kao LC. Endometriosis. *Lancet*. 2004;364(9447):1789-99. Epub 2004/11/16.
2. Eskenazi B, Warner ML. Epidemiology of endometriosis. *Obstetrics and gynecology clinics of North America*. 1997;24(2):235-58. Epub 1997/06/01.
3. Stilley JA, Birt JA, Sharpe-Timms KL. Cellular and molecular basis for endometriosis-associated infertility. *Cell and tissue research*. 2012;349(3):849-62. Epub 2012/02/03.
4. Asante A, Taylor RN. Endometriosis: the role of neuroangiogenesis. *Annual review of physiology*. 2011;73:163-82. Epub 2010/11/09.
5. Fauconnier A, Chapron C. Endometriosis and pelvic pain: epidemiological evidence of the relationship and implications. *Human reproduction update*. 2005;11(6):595-606. Epub 2005/09/21.
6. Simoens S, Dunselman G, Dirksen C, Hummelshoj L, Bokor A, Brandes I, et al. The burden of endometriosis: costs and quality of life of women with endometriosis and treated in referral centres. *Hum Reprod*. 2012;27(5):1292-9. Epub 2012/03/17.
7. Rogers PA, D'Hooghe TM, Fazleabas A, Gargett CE, Giudice LC, Montgomery GW, et al. Priorities for endometriosis research: recommendations from an international consensus workshop. *Reprod Sci*. 2009;16(4):335-46. Epub 2009/02/07.
8. Kennedy S, Bergqvist A, Chapron C, D'Hooghe T, Dunselman G, Greb R, et al. ESHRE guideline for the diagnosis and treatment of endometriosis. *Hum Reprod*. 2005;20(10):2698-704. Epub 2005/06/28.
9. Vinatier D, Orazi G, Cosson M, Dufour P. Theories of endometriosis. *European journal of obstetrics, gynecology, and reproductive biology*. 2001;96(1):21-34. Epub 2001/04/20.
10. Sampson JA. Metastatic or Embolic Endometriosis, due to the Menstrual Dissemination of Endometrial Tissue into the Venous Circulation. *The American journal of pathology*. 1927;3(2):93-110 43. Epub 1927/03/01.
11. Olive DL, Henderson DY. Endometriosis and mullerian anomalies. *Obstetrics and gynecology*. 1987;69(3 Pt 1):412-5. Epub 1987/03/01.
12. D'Hooghe TM, Bambra CS, Suleman MA, Dunselman GA, Evers HL, Koninckx PR. Development of a model of retrograde menstruation in baboons (*Papio anubis*). *Fertility and sterility*. 1994;62(3):635-8. Epub 1994/09/01.
13. Halme J, Hammond MG, Hulka JF, Raj SG, Talbert LM. Retrograde menstruation in healthy women and in patients with endometriosis. *Obstetrics and gynecology*. 1984;64(2):151-4. Epub 1984/08/01.
14. Van Schil PE, Vercauteren SR, Vermeire PA, Nackaerts YH, Van Marck EA. Catamenial pneumothorax caused by thoracic endometriosis. *The Annals of thoracic surgery*. 1996;62(2):585-6. Epub 1996/08/01.
15. Rosenfeld DL, Lecher BD. Endometriosis in a patient with Rokitansky-Kuster-Hauser syndrome. *American journal of obstetrics and gynecology*. 1981;139(1):105. Epub 1981/01/01.
16. El-Mahgoub S, Yaseen S. A positive proof for the theory of coelomic metaplasia. *American journal of obstetrics and gynecology*. 1980;137(1):137-40. Epub 1980/05/01.
17. Schrodt GR, Alcorn MO, Ibanez J. Endometriosis of the male urinary system: a case report. *The Journal of urology*. 1980;124(5):722-3. Epub 1980/11/01.
18. Clark AH. Endometriosis in a young girl. *Journal of the American Medical Association*. 1948;136(10):690. Epub 1948/03/06.
19. Nakamura M, Katabuchi H, Tohya T, Fukumatsu Y, Matsuura K, Okamura H. Scanning electron microscopic and immunohistochemical studies of pelvic endometriosis. *Hum Reprod*. 1993;8(12):2218-26. Epub 1993/12/01.
20. Burney RO, Giudice LC. Pathogenesis and pathophysiology of endometriosis. *Fertility and sterility*. 2012;98(3):511-9. Epub 2012/07/24.
21. Missmer SA, Hankinson SE, Spiegelman D, Barbieri RL, Michels KB, Hunter DJ. In utero exposures and the incidence of endometriosis. *Fertility and sterility*. 2004;82(6):1501-8. Epub 2004/12/14.
22. Sasson IE, Taylor HS. Stem cells and the pathogenesis of endometriosis. *Annals of the New York Academy of Sciences*. 2008;1127:106-15. Epub 2008/04/30.

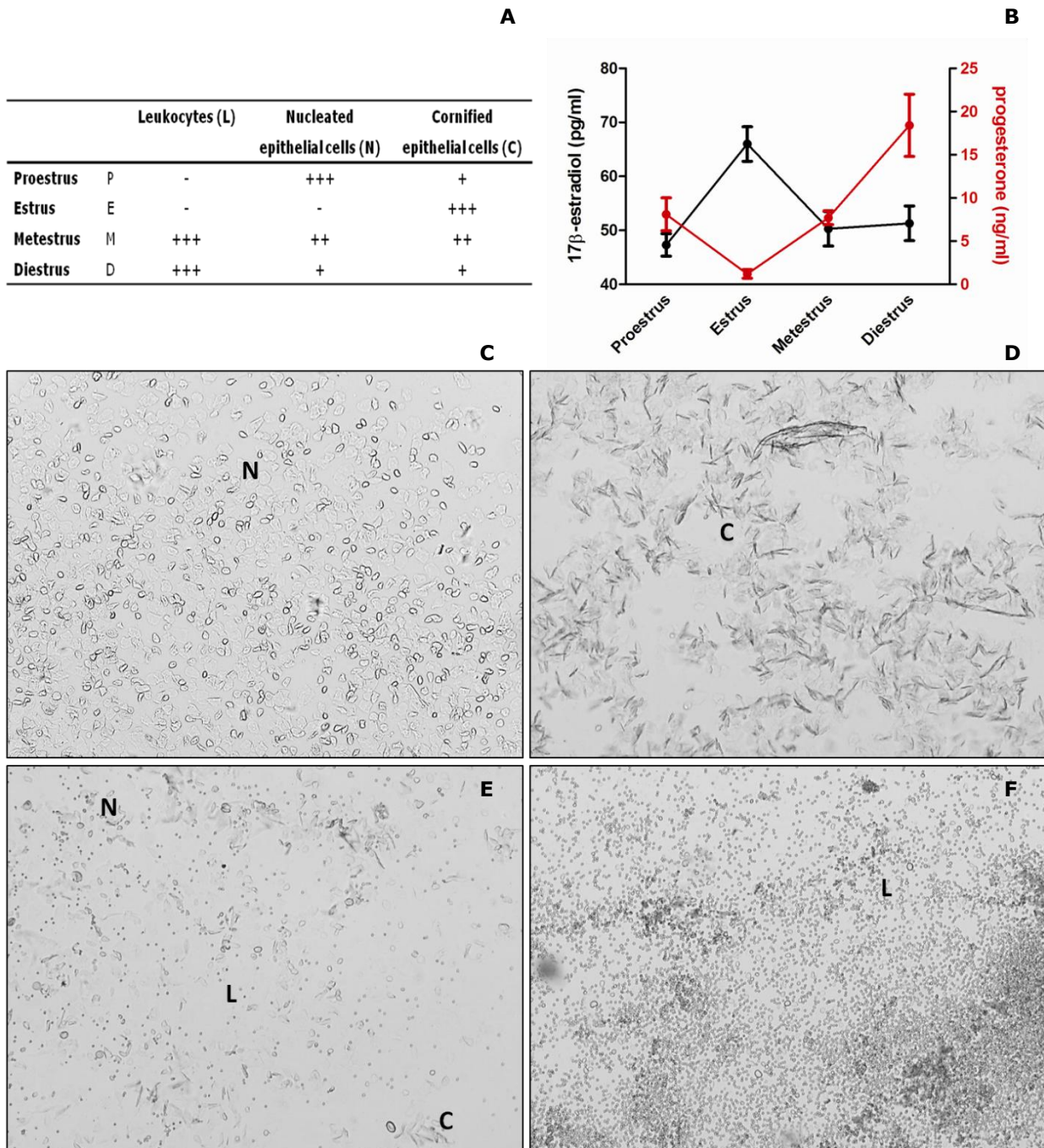
23. Figueira PG, Abrao MS, Krikun G, Taylor HS. Stem cells in endometrium and their role in the pathogenesis of endometriosis. *Annals of the New York Academy of Sciences*. 2011;1221:10-7. Epub 2011/03/16.
24. Taniguchi F, Kaponis A, Izawa M, Kiyama T, Deura I, Ito M, et al. Apoptosis and endometriosis. *Front Biosci (Elite Ed)*. 2011;3:648-62. Epub 2011/01/05.
25. Augoulea A, Alexandrou A, Creatsa M, Vrachnis N, Lambrinouadaki I. Pathogenesis of endometriosis: the role of genetics, inflammation and oxidative stress. *Archives of gynecology and obstetrics*. 2012;286(1):99-103. Epub 2012/05/02.
26. Nyholt DR, Low SK, Anderson CA, Painter JN, Uno S, Morris AP, et al. Genome-wide association meta-analysis identifies new endometriosis risk loci. *Nature genetics*. 2012;44(12):1355-9. Epub 2012/10/30.
27. Kyama CM, Debrock S, Mwenda JM, D'Hooghe TM. Potential involvement of the immune system in the development of endometriosis. *Reproductive biology and endocrinology : RB&E*. 2003;1:123. Epub 2003/12/04.
28. Witz CA, Thomas MR, Montoya-Rodriguez IA, Nair AS, Centonze VE, Schenken RS. Short-term culture of peritoneum explants confirms attachment of endometrium to intact peritoneal mesothelium. *Fertility and sterility*. 2001;75(2):385-90. Epub 2001/02/15.
29. Lucidi RS, Witz CA, Chrisco M, Binkley PA, Shain SA, Schenken RS. A novel in vitro model of the early endometriotic lesion demonstrates that attachment of endometrial cells to mesothelial cells is dependent on the source of endometrial cells. *Fertility and sterility*. 2005;84(1):16-21. Epub 2005/07/13.
30. Giudice LC. Genomics' role in understanding the pathogenesis of endometriosis. *Seminars in reproductive medicine*. 2003;21(2):119-24. Epub 2003/08/15.
31. Jensen JR, Coddington CC, 3rd. Evolving spectrum: the pathogenesis of endometriosis. *Clinical obstetrics and gynecology*. 2010;53(2):379-88. Epub 2010/05/04.
32. Kitawaki J, Kado N, Ishihara H, Koshiha H, Kitaoka Y, Honjo H. Endometriosis: the pathophysiology as an estrogen-dependent disease. *The Journal of steroid biochemistry and molecular biology*. 2002;83(1-5):149-55. Epub 2003/03/26.
33. Zeitoun K, Takayama K, Sasano H, Suzuki T, Moghrabi N, Andersson S, et al. Deficient 17beta-hydroxysteroid dehydrogenase type 2 expression in endometriosis: failure to metabolize 17beta-estradiol. *The Journal of clinical endocrinology and metabolism*. 1998;83(12):4474-80. Epub 1998/12/16.
34. Noble LS, Simpson ER, Johns A, Bulun SE. Aromatase expression in endometriosis. *The Journal of clinical endocrinology and metabolism*. 1996;81(1):174-9. Epub 1996/01/01.
35. Taylor RN, Yu J, Torres PB, Schickedanz AC, Park JK, Mueller MD, et al. Mechanistic and therapeutic implications of angiogenesis in endometriosis. *Reprod Sci*. 2009;16(2):140-6. Epub 2008/11/13.
36. Nisolle M, Casanas-Roux F, Anaf V, Mine JM, Donnez J. Morphometric study of the stromal vascularization in peritoneal endometriosis. *Fertility and sterility*. 1993;59(3):681-4. Epub 1993/03/01.
37. Reichelt U, Keichel S, Barcena de Arellano ML, Chiantera V, Schneider A, Mechsner S. High lymph vessel density and expression of lymphatic growth factors in peritoneal endometriosis. *Reprod Sci*. 2012;19(8):876-82. Epub 2012/04/28.
38. Tokushige N, Markham R, Russell P, Fraser IS. Nerve fibres in peritoneal endometriosis. *Hum Reprod*. 2006;21(11):3001-7. Epub 2006/09/05.
39. Stratton P, Berkley KJ. Chronic pelvic pain and endometriosis: translational evidence of the relationship and implications. *Human reproduction update*. 2011;17(3):327-46. Epub 2010/11/26.
40. Attia GR, Zeitoun K, Edwards D, Johns A, Carr BR, Bulun SE. Progesterone receptor isoform A but not B is expressed in endometriosis. *The Journal of clinical endocrinology and metabolism*. 2000;85(8):2897-902. Epub 2000/08/18.
41. Burney RO, Lathi RB. Menstrual bleeding from an endometriotic lesion. *Fertil Steril*. 2009;91(5):1926-7. Epub 2008/10/22.
42. Jenkins S, Olive DL, Haney AF. Endometriosis: pathogenetic implications of the anatomic distribution. *Obstetrics and gynecology*. 1986;67(3):335-8. Epub 1986/03/01.

43. Ito S, Okuda-Ashitaka E, Minami T. Central and peripheral roles of prostaglandins in pain and their interactions with novel neuropeptides nociceptin and nocistatin. *Neuroscience research*. 2001;41(4):299-332. Epub 2002/01/05.
44. Taylor-Clark TE, Undem BJ, Macglashan DW, Jr., Ghatta S, Carr MJ, McAlexander MA. Prostaglandin-induced activation of nociceptive neurons via direct interaction with transient receptor potential A1 (TRPA1). *Molecular pharmacology*. 2008;73(2):274-81. Epub 2007/11/15.
45. Revised American Society for Reproductive Medicine classification of endometriosis: 1996. *Fertility and sterility*. 1997;67(5):817-21. Epub 1997/05/01.
46. Brosens I, Puttemans P, Campo R, Gordts S, Kinkel K. Diagnosis of endometriosis: pelvic endoscopy and imaging techniques. *Best practice & research Clinical obstetrics & gynaecology*. 2004;18(2):285-303. Epub 2004/05/26.
47. Sinaii N, Plumb K, Cotton L, Lambert A, Kennedy S, Zondervan K, et al. Differences in characteristics among 1,000 women with endometriosis based on extent of disease. *Fertility and sterility*. 2008;89(3):538-45. Epub 2007/05/15.
48. Olive DL, Pritts EA. Treatment of endometriosis. *The New England journal of medicine*. 2001;345(4):266-75. Epub 2001/07/28.
49. Olive DL, Lindheim SR, Pritts EA. New medical treatments for endometriosis. *Best practice & research Clinical obstetrics & gynaecology*. 2004;18(2):319-28. Epub 2004/05/26.
50. D'Hooghe TM, Kyama CM, Chai D, Fassbender A, Vodolazkaia A, Bokor A, et al. Nonhuman primate models for translational research in endometriosis. *Reprod Sci*. 2009;16(2):152-61. Epub 2009/02/12.
51. Pullen N, Birch CL, Douglas GJ, Hussain Q, Pruimboom-Brees I, Walley RJ. The translational challenge in the development of new and effective therapies for endometriosis: a review of confidence from published preclinical efficacy studies. *Human reproduction update*. 2011;17(6):791-802. Epub 2011/07/08.
52. Tirado-Gonzalez I, Barrientos G, Tariverdian N, Arck PC, Garcia MG, Klapp BF, et al. Endometriosis research: animal models for the study of a complex disease. *Journal of reproductive immunology*. 2010;86(2):141-7. Epub 2010/07/03.
53. Kling OR, Westfahl PK. Steroid changes during the menstrual cycle of the baboon (*Papio cynocephalus*) and human. *Biology of reproduction*. 1978;18(3):392-400. Epub 1978/04/01.
54. Story L, Kennedy S. Animal studies in endometriosis: a review. *ILAR journal / National Research Council, Institute of Laboratory Animal Resources*. 2004;45(2):132-8. Epub 2004/04/28.
55. Grummer R. Animal models in endometriosis research. *Human reproduction update*. 2006;12(5):641-9. Epub 2006/06/16.
56. Rudolph M, Docke WD, Muller A, Menning A, Rose L, Zollner TM, et al. Induction of overt menstruation in intact mice. *PloS one*. 2012;7(3):e32922. Epub 2012/03/14.
57. Menning A, Walter A, Rudolph M, Gashaw I, Fritzscheier KH, Roesel L. Granulocytes and vascularization regulate uterine bleeding and tissue remodeling in a mouse menstruation model. *PloS one*. 2012;7(8):e41800. Epub 2012/08/11.
58. Wood GA, Fata JE, Watson KL, Khokha R. Circulating hormones and estrous stage predict cellular and stromal remodeling in murine uterus. *Reproduction*. 2007;133(5):1035-44. Epub 2007/07/10.
59. Cheng CW, Licence D, Cook E, Luo F, Arends MJ, Smith SK, et al. Activation of mutated K-ras in donor endometrial epithelium and stroma promotes lesion growth in an intact immunocompetent murine model of endometriosis. *The Journal of pathology*. 2011;224(2):261-9. Epub 2011/04/12.
60. Finn CA, Pope M. Vascular and cellular changes in the decidualized endometrium of the ovariectomized mouse following cessation of hormone treatment: a possible model for menstruation. *The Journal of endocrinology*. 1984;100(3):295-300. Epub 1984/03/01.
61. Brasted M, White CA, Kennedy TG, Salamonsen LA. Mimicking the events of menstruation in the murine uterus. *Biology of reproduction*. 2003;69(4):1273-80. Epub 2003/06/13.

62. Xu XB, He B, Wang JD. Menstrual-like changes in mice are provoked through the pharmacologic withdrawal of progesterone using mifepristone following induction of decidualization. *Hum Reprod.* 2007;22(12):3184-91. Epub 2007/10/09.
63. Kaitu'u-Lino TJ, Ye L, Salamonsen LA, Girling JE, Gargett CE. Identification of label-retaining perivascular cells in a mouse model of endometrial decidualization, breakdown, and repair. *Biology of reproduction.* 2012;86(6):184. Epub 2012/03/10.
64. Kaitu'u TJ, Shen J, Zhang J, Morison NB, Salamonsen LA. Matrix metalloproteinases in endometrial breakdown and repair: functional significance in a mouse model. *Biology of reproduction.* 2005;73(4):672-80. Epub 2005/06/10.
65. Caligioni CS. Assessing reproductive status/stages in mice. *Current protocols in neuroscience / editorial board, Jacqueline N Crawley [et al].* 2009;Appendix 4:Appendix 4I. Epub 2009/07/04.
66. Milligan SR, Cohen PE. Silastic implants for delivering physiological concentrations of progesterone to mice. *Reproduction, fertility, and development.* 1994;6(2):235-9. Epub 1994/01/01.
67. Molinas CR, Mynbaev O, Pauwels A, Novak P, Koninckx PR. Peritoneal mesothelial hypoxia during pneumoperitoneum is a cofactor in adhesion formation in a laparoscopic mouse model. *Fertil Steril.* 2001;76(3):560-7. Epub 2001/09/05.
68. Dixon WJ. Efficient analysis of experimental observations. *Annual review of pharmacology and toxicology.* 1980;20:441-62. Epub 1980/01/01.
69. Bokor A, Kyama CM, Vercruyssen L, Fassbender A, Gevaert O, Vodolazkaia A, et al. Density of small diameter sensory nerve fibres in endometrium: a semi-invasive diagnostic test for minimal to mild endometriosis. *Hum Reprod.* 2009;24(12):3025-32. Epub 2009/08/20.
70. Wang Q, Xu X, He B, Li Y, Chen X, Wang J. A critical period of progesterone withdrawal precedes endometrial breakdown and shedding in mouse menstrual-like model. *Hum Reprod.* 2013;28(6):1670-8. Epub 2013/03/21.
71. D'Hooghe TM, Bambra CS, Raeymaekers BM, De Jonge I, Lauweryns JM, Koninckx PR. Intrapelvic injection of menstrual endometrium causes endometriosis in baboons (*Papio cynocephalus* and *Papio anubis*). *American journal of obstetrics and gynecology.* 1995;173(1):125-34. Epub 1995/07/01.
72. Thompson RJ, Doran JF, Jackson P, Dhillon AP, Rode J. PGP 9.5--a new marker for vertebrate neurons and neuroendocrine cells. *Brain research.* 1983;278(1-2):224-8. Epub 1983/11/14.
73. Yamashita S. Heat-induced antigen retrieval: mechanisms and application to histochemistry. *Progress in histochemistry and cytochemistry.* 2007;41(3):141-200. Epub 2007/01/02.
74. Leong TY, Cooper K, Leong AS. Immunohistochemistry--past, present, and future. *Advances in anatomic pathology.* 2010;17(6):404-18. Epub 2010/10/23.
75. Emoto K, Yamashita S, Okada Y. Mechanisms of heat-induced antigen retrieval: does pH or ionic strength of the solution play a role for refolding antigens? *The journal of histochemistry and cytochemistry : official journal of the Histochemistry Society.* 2005;53(11):1311-21. Epub 2005/07/13.
76. Schrenzel M, Oaks JL, Rotstein D, Maalouf G, Snook E, Sandfort C, et al. Characterization of a new species of adenovirus in falcons. *Journal of clinical microbiology.* 2005;43(7):3402-13. Epub 2005/07/08.
77. Green BG, Roman C, Schoen K, Collins H. Nociceptive sensations evoked from 'spots' in the skin by mild cooling and heating. *Pain.* 2008;135(1-2):196-208. Epub 2008/01/16.
78. Vriens J, Owsianik G, Hofmann T, Philipp SE, Stab J, Chen X, et al. TRPM3 is a nociceptor channel involved in the detection of noxious heat. *Neuron.* 2011;70(3):482-94. Epub 2011/05/11.
79. Dhaka A, Murray AN, Mathur J, Earley TJ, Petrus MJ, Patapoutian A. TRPM8 is required for cold sensation in mice. *Neuron.* 2007;54(3):371-8. Epub 2007/05/08.
80. Yu L, Yang F, Luo H, Liu FY, Han JS, Xing GG, et al. The role of TRPV1 in different subtypes of dorsal root ganglion neurons in rat chronic inflammatory nociception induced by complete Freund's adjuvant. *Molecular pain.* 2008;4:61. Epub 2008/12/06.

81. He W, Liu X, Zhang Y, Guo SW. Generalized hyperalgesia in women with endometriosis and its resolution following a successful surgery. *Reprod Sci.* 2010;17(12):1099-111. Epub 2010/10/07.
82. Fata JE, Chaudhary V, Khokha R. Cellular turnover in the mammary gland is correlated with systemic levels of progesterone and not 17beta-estradiol during the estrous cycle. *Biology of reproduction.* 2001;65(3):680-8. Epub 2001/08/22.
83. Gilbert SF. *Developmental biology.* 9th ed. Sunderland, Mass.: Sinauer Associates; 2010. xxi, 711, 80 p. p.

Supplemental information



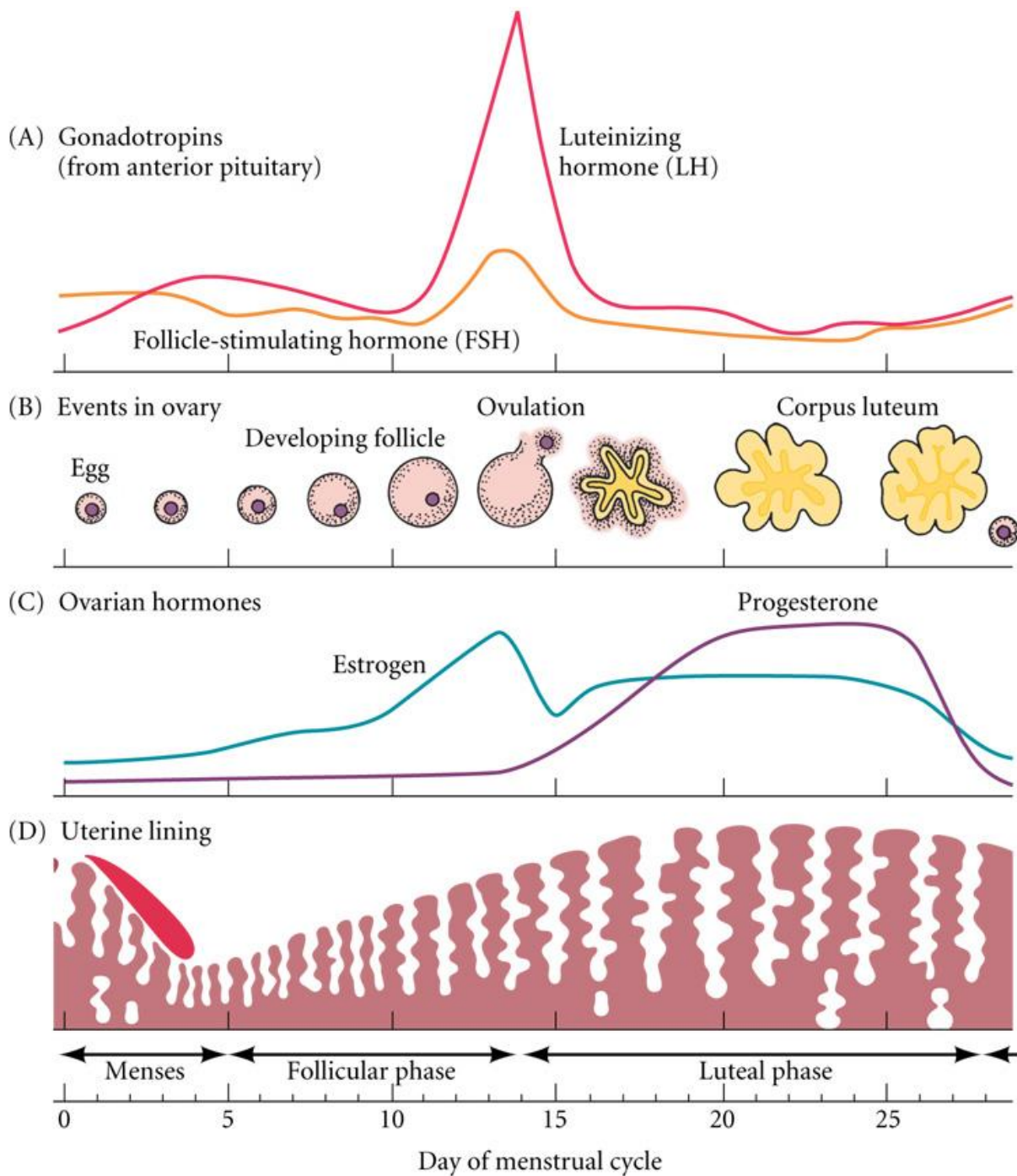
Supplementary data figure 1: **The estrous cycle of mice.** **A.** Listing of the three different cell types that are present during the stages of the estrous cycle. **B.** Fluctuations in hormonal concentration of 17β-estradiol (pg/ml) and progesterone (ng/ml) during the estrous cycle as described by *Fata et al* (82). Photomicrograph of unstained vaginal smear from mice at proestrus, indicating the predominance of nucleated epithelial cells (**C**); estrus, consisting of cornified epithelial cells (**D**); metestrus, displaying all three cell types, leukocytes, nucleated and cornified epithelial cells (**E**); and diestrus illustrating the predominance of leukocytes (**F**). Pictures were taken at 10x objective without the use of a condenser lens, description of estrous cycle was adopted from *Caligioni* (65) [L: leukocytes, N: nucleated epithelial cells, C: cornified epithelial cells].

Supplementary data table 1: **Estrous cycle of the animals during the protocol of the menstruating mouse model.**

	Ove x	100 E2	100 E2	100 E2										5 E2 + P4	5 E2 + P4	5 E2 + P4	P4	P4	P4	P4
Day	-6	-5	-4	-3	-2	-1	0	1	2	3	4	5	6	7	8	9	10	11	12	13
Animal																				
1	D	M/D	D	D	D	M	D	M	M	P	E/M	E/M	E/M	M/D	D	D	D	M/D	M/D	M/D
2	M/D	E/M	E	E/M	D	M	M	D	M	P/E	M	E	M	M	M	M/D	M/D	M/D	D	D
3	M	E	E	M	M	M	M	M	M	P	E	E	M	M	D	M/D	M	D	D	M/D
4	D	M	P/E	M	M	M	M	M	M	P/E	E	E	M	M/D	D	D	M	M	D	M/D
7	E	E	E/M	DM/	M/D	M	M	M/D	M	P	E	E/M	E/M	M/D	M/D	D	D	D	D	M/D
8	E	E/M	M/D	D	M	M	D	M/D	D	D/P	E/M	E/M	EM/	E/M	M/E	D	M/D	M/D	M	D
9	E	D	D	D	D	M	D	D	D/P	E	E	E	M	D	D	D	D	D	D	M/D
11	E	M/D	D	D	M	M	M	M	M	E/M	E/M	E/M	E/M	M	M	D	M/D	D	M	D
12	E	D	E/M	M	M	D	M	M	M/D	P/E	E/M	E/M	E/M	M	M	D	D	M	M	M
13	E	M	M/P	M	M	M	D	M	D	P/E	E/M	E/M	E/M	M/D	M/D	D	D	M	M	M
14	E	E	M	D	M	M	M	M	D	P	E	E	M	D	M/D	M/D	M	M	M	M/D
15	M	E	E	E/M	M	M	M	M	D	P	E/M	E/M	E	M/D	M/D	D	D	D	M/D	D
16	M	M	M	M	D	D/P	M	D	M	P/E	E	E/M	M	M	M	D	D	D	D	D
18	M	M	P	E	M	D	M	D	M	P/E	E	E	M	D	D	M	M	M	D	M
20	E	M	M/D	M/D	D	D	M	D	M	P	E/M	E/M	M	M	M	M	D	D	D	M/D
21	E	E	M	M	D	D	M	M/D	D	P/E	E/M	E/M	M	M	M	M/D	M/D	D	D	D
22	E	E	E	M	D	M/D	D	M	M	P/E	E	E	M	M	D	D	M	M/D	M	M
23	M	M/D	M	D	M	D	D	D	D	P/E	E/M	E	M/E	M/D	D	D	M	D	M	D
24	D	D	D	D	D	D	M/D	E	M	P/E	E/M	E/M	M	M	M	M	M	D	D	M
26	M	E/M	E/M	E/M	M	M/D	M/D	M	M	P/E	E/M	E/M	E/M	M/D	D	D	D	D	D	D
27	M	M	M	D	M/D	D	D	D	M	P/E	E/M	E/M	E/M	M/D	M/D	D	D	M/D	M/D	M/D
28	D/P	M/D	M	M	M	M	M	M	M	P	E/M	E	E/M	E/M	M	D	M	D	D	D
29	E	E	M	D	M/D	M	M	M	M	P/E	E	E	M/D	M/D	D	D	M	M	D	D
30	M	E	E	M	M/D	D	D	M	D	P/E	E/M	E/M	E/M	M	M/D	M/D	D	D	D	M/D
31	E/M	D	M	M	M	M	M	M	M	P/E	E/M	E/M	E/M	M/D	M/D	D	M	M	M/D	M

32	M	E	M	D	D	D	M/D	M/D	M	P	E	E/M	E/M	M	M	M	M	D	D	D
33	E	M	M	M/D	M/D	M/D	M	M	M	P/E	E/M	E	E/M	M/D	M/D	D	M/D	M/D	M	M
34	E	E/M	M	D	M	M	M	M	M/D	P	E/M	E/M	E/M	M/D	M/D	D	D	M/D	D	D
35	E	M	M/D	D	D/M	M	M	M	M/D	P/E	E/M	E/M	M	M	M/D	D	M/D	M	D	M/D
36	M	M	M	M/D	D	M	M	M	M/D	P	E/M	E/M	E/M	M/D	E/M	M/D	D	D	D	M/D
37	D	M	P/E	E	M	M	M	D	M	P/E	E	E	M	M	D	M	M	M	D	M
38	P/E	E	E	E/M	D	D	M	D	M	D/P	E/M	E/M	E/M	M	M	M	M/D	D	D	M
39	E	E	M	M	M	M	M	M/D	D	P	E/M	E	M	M/D	D	D	D	D	M/D	D
40	M	M	E/M	M	M	M	M	M	M	P/E	E/M	E/M	E	M	M	D	D	M/D	M/D	M/D

Staging of the cycle was performed daily by applying 50µl of PBS into the vagina of the animals and flushing three times. Hereafter, the vaginal flush was collected and microscopically examined. During the protocol of the menstruating mouse model, the animals were subjected to 100ng injections of E2 (100 E2), 5ng injections of E2 (5 E2) and a P4 pellet (P4). Only animals that survived the whole menstruating protocol are included in this table. When the animal resided between two cycles, both cycles were recorded attached by a dash [E2: 17β-estradiol, P4: progesterone, ovex: ovariectomy, P: proestrus, E: estrus, M: metestrus, D: diestrus].



Supplementary data figure 2: **Human menstrual cycle.** Different aspects of the human menstrual cycle, including the gonadotropin levels (A), the events in the ovaries (B), the ovarian hormone course (C) and the changes in uterine lining (D). Picture was taken from Gilbert (83).

Auteursrechtelijke overeenkomst

Ik/wij verlenen het wereldwijde auteursrecht voor de ingediende eindverhandeling:

**
The menstruating mouse model for preclinical endometriosis research
Optimization of the decidualization process, nerve fiber detection and nocifensive behavior identification**

Richting: **master in de biomedische wetenschappen-klinische en moleculaire wetenschappen**

Jaar: **2013**

in alle mogelijke mediaformaten, - bestaande en in de toekomst te ontwikkelen - , aan de Universiteit Hasselt.

Niet tegenstaand deze toekenning van het auteursrecht aan de Universiteit Hasselt behoud ik als auteur het recht om de eindverhandeling, - in zijn geheel of gedeeltelijk -, vrij te reproduceren, (her)publiceren of distribueren zonder de toelating te moeten verkrijgen van de Universiteit Hasselt.

Ik bevestig dat de eindverhandeling mijn origineel werk is, en dat ik het recht heb om de rechten te verlenen die in deze overeenkomst worden beschreven. Ik verklaar tevens dat de eindverhandeling, naar mijn weten, het auteursrecht van anderen niet overtreedt.

Ik verklaar tevens dat ik voor het materiaal in de eindverhandeling dat beschermd wordt door het auteursrecht, de nodige toelatingen heb verkregen zodat ik deze ook aan de Universiteit Hasselt kan overdragen en dat dit duidelijk in de tekst en inhoud van de eindverhandeling werd genotificeerd.

Universiteit Hasselt zal mij als auteur(s) van de eindverhandeling identificeren en zal geen wijzigingen aanbrengen aan de eindverhandeling, uitgezonderd deze toegelaten door deze overeenkomst.

Voor akkoord,

Goossens, Chloë